1882

Geology and Geochemistry of Synsedimentary Cobaltiferous-Pyrite Deposits, Iron Creek, Lemhi County, Idaho

U.S. GEOLOGICAL SURVEY BULLETIN 1882

I 19.3:

READEX FICHE best copy available

AVAILABILITY OF BOOKS AND MAPS OF THE U.S. GEOLOGICAL SURVEY

Instructions on ordering publications of the U.S. Geological Survey, along with prices of the last offerings, are given in the current-year issues of the monthly catalog "New Publications of the U.S. Geological Survey." Prices of available U.S. Geological Survey publications released prior to the current year are listed in the most recent annual "Price and Availability List." Publications that are listed in various U.S. Geological Survey catalogs (see back inside cover) but not listed in the most recent annual "Price and Availability List" are no longer available.

Prices of reports released to the open files are given in the listing "U.S. Geological Survey Open-File Reports," updated monthly, which is for sale in microfiche from the U.S. Geological Survey, Books and Open-File Reports Section, Federal Center, Box 25425, Denver, CO 80225. Reports released through the NTIS may be obtained by writing to the National Technical Information Service, U.S. Department of Commerce, Springfield, VA 22161; please include NTIS report number with inquiry.

Order U.S. Geological Survey publications **by mail** or **over the counter** from the offices given below.

BY MAIL

Books

Professional Papers, Bulletins, Water-Supply Papers, Techniques of Water-Resources Investigations, Circulars, publications of general interest (such as leaflets, pamphlets, booklets), single copies of Earthquakes & Volcanoes, Preliminary Determination of Epicenters, and some miscellaneous reports, including some of the foregoing series that have gone out of print at the Superintendent of Documents, are obtainable by mail from

U.S. Geological Survey, Books and Open-File Reports
Federal Center, Box 25425
Denver, CO 80225

Subscriptions to periodicals (Earthquakes & Volcanoes and Preliminary Determination of Epicenters) can be obtained ONLY from the

Superintendent of Documents
Government Printing Office
Washington, D.C. 20402

(Check or money order must be payable to Superintendent of Documents.)

Maps

For maps, address mail orders to

U.S. Geological Survey, Map Distribution
Federal Center, Box 25286
Denver, CO 80225

Residents of Alaska may order maps from

Alaska Distribution Section, U.S. Geological Survey,
New Federal Building - Box 12
101 Twelfth Ave., Fairbanks, AK 99701

OVER THE COUNTER

Books

Books of the U.S. Geological Survey are available over the counter at the following Geological Survey Public Inquiries Offices, all of which are authorized agents of the Superintendent of Documents:

- **WASHINGTON, D.C.**--Main Interior Bldg., 2600 corridor, 18th and C Sts., NW.
- **DENVER, Colorado**--Federal Bldg., Rm. 169, 1961 Stout St.
- **LOS ANGELES, California**--Federal Bldg., Rm. 7638, 300 N. Los Angeles St.
- **MENLO PARK, California**--Bldg. 3 (Stop 533), Rm. 3128, 345 Middlefield Rd.
- **RESTON, Virginia**--503 National Center, Rm. 1C402, 12201 Sunrise Valley Dr.
- **SALT LAKE CITY, Utah**--Federal Bldg., Rm. 8105, 125 South State St.
- **SAN FRANCISCO, California**--Customhouse, Rm. 504, 555 Battery St.
- **SPOKANE, Washington**--U.S. Courthouse, Rm. 678, West 920 Riverside Ave..
- **ANCHORAGE, Alaska**--Rm. 101, 4230 University Dr.
- **ANCHORAGE, Alaska**--Federal Bldg, Rm. E-146, 701 C St.

Maps

Maps may be purchased over the counter at the U.S. Geological Survey offices where books are sold (all addresses in above list) and at the following Geological Survey offices:

- **ROLLA, Missouri**--1400 Independence Rd.
- **DENVER, Colorado**--Map Distribution, Bldg. 810, Federal Center
- **FAIRBANKS, Alaska**--New Federal Bldg., 101 Twelfth Ave.

Geology and Geochemistry of Synsedimentary Cobaltiferous-Pyrite Deposits, Iron Creek, Lemhi County, Idaho

By J. THOMAS NASH

A description of cobaltiferous-pyrite lenses in Precambrian metasedimentary rocks that are partly stratiform and partly discordant in zones of soft-sediment deformation

U.S. GEOLOGICAL SURVEY BULLETIN 1882

DEPARTMENT OF THE INTERIOR
MANUEL LUJAN, JR., Secretary

U. S. GEOLOGICAL SURVEY
Dallas L. Peck, Director

Any use of trade, product, or firm names in this publication is for descriptive purposes only and does not imply endorsement by the U.S. Government.

UNITED STATES GOVERNMENT PRINTING OFFICE: 1989

For sale by the
Books and Open-File Reports Section
U.S. Geological Survey
Federal Center
Box 25425
Denver, CO 80225

Library of Congress Cataloging-in-Publication Data

Nash, J. Thomas (John Thomas), 1941–
Geology and geochemistry of synsedimentary cobaltiferous-pyrite deposits, Iron Creek, Lemhi County, Idaho / by J. Thomas Nash.
p. cm.—(U.S. Geological Survey bulletin ; 1882)
"A description of cobaltiferous-pyrite lenses in Precambrian metasedimentary rocks that are partly stratiform and partly discordant in zones of soft-sediment deformation."
Bibliography: p.
Supt. of Docs. no.: I 19.3:1882
1. Cobalt ores —Idaho—Iron Creek Region (Lemhi County)
2. Pyrites—Idaho—Iron Creek Region (Lemhi County)
3. Geology—Idaho—Iron Creek Region (Lemhi County) 4. Geology, Stratigraphic—Pre-Cambrian. I. Title. II. Series.
QE75.B9 no. 1882
[QE390.2.C58]
557.3 s —dc19
[553.4'8]

89–600025
CIP

CONTENTS

Abstract 1
Introduction 1
Previous exploration and geologic studies 3
    Geophysics 3
    Geology 3
Geochemical methods 5
Geologic setting 5
    Stratigraphy 5
    Structure 6
Jackass zone 6
The No-Name deposit 9
    Structure 9
    Lithology 9
    Soft-sediment deformation 11
    Ore mineralogy 14
    Alteration 14
Geochemistry 15
Discussion and interpretation 23
    Environment of formation 23
    Synsedimentary structural controls 23
    Geochemistry 24
    Similar ore deposits 24
    Metamorphism 25
    Resources and exploration 25
    Ore genesis 26
References cited 26
Appendix 1. Description of analyzed samples 30
Appendix 2. Methods for geochemical analysis 32

FIGURES

1. Map showing location of Iron Creek area in Idaho cobalt belt 2
2. Map showing generalized geology of Iron Creek area and location of mineralized zones 4
3. Generalized lithologic logs of drill holes through the No-Name deposit showing distribution of disruption zones, cobalt, and copper 7
4. Photographs of drill core from the Yellowjacket Formation showing disruption structures 8
5. Photographs of thin sections showing textures of sedimentary rocks from the Yellowjacket Formation 10
6. Photomicrographs of textures in thin sections of samples from the Yellowjacket Formation 12
7. Scatterplots of geochemical data for the No-Name deposit 22

TABLES

1. Analytical results for samples of drill core from the No-Name deposit 16
2. Summary of analytical results for ore and enclosing wallrocks, No-Name deposit 21
3. Lower limits of determination in geochemical analyses of samples from the No-Name deposit 33

Geology and Geochemistry of Synsedimentary Cobaltiferous-Pyrite Deposits, Iron Creek, Lemhi County, Idaho

By J. Thomas Nash

Abstract

Cobaltiferous-pyrite deposits at the No-Name prospect occur in weakly metamorphosed argillite and siltite of the Middle Proterozoic Yellowjacket Formation, about 28 km southwest of Salmon, Idaho. The No-Name deposit comprises several lenses of stratiform and discordant pyrite in a zone as much as 250 m thick and more than 1,500 m long. Cobalt grades typically are in the range 0.2–0.7 percent, some intercepts being in excess of 1 percent, along with copper in the range 0.5–1 percent. Two stratabound zones of iron-rich mineralized rock are known in the area, of which the stratigraphically lower one contains chiefly magnetite having generally low sulfide and cobalt content. The No-Name deposit contains abundant magnetite at the bottom and pyrite and chalcopyrite in upper layers. Approximately equal amounts of fine-grained stratiform pyrite and coarse-grained epigenetic pyrite are present, and most of the cobalt is contributed by the epigenetic variety. The cobalt-copper zones are associated with synsedimentary disruption structures characterized by retextured sediment, loss of bedding features, lump breccia, and probable bedding-plane slips—all probably produced by liquefaction, fluidization, and submarine sliding of unconsolidated sediment. The pyrite deposits are enriched in Fe, S, As, Ba, Bi, Co, Cr, Cu, Ni, Pb, Se, and Zn, but the concentrations of Ag, Pb, and Zn are much lower than in most sediment-hosted base-metal deposits. Arsenic content is much lower than in the Blackbird deposits, 30 km to the northwest, which greatly simplifies the metallurgy of these sulfide concentrates.

The cobaltiferous-pyrite deposits formed in a submarine geothermal system associated with rifting and volcanism in the Yellowjacket basin. Geothermal vents in this part of the rift basin are marked by lenses of magnetite iron-formation, and the No-Name system evolved to one that deposited syngenetic and epigenetic iron and copper sulfide minerals. Syngenetic pyrite contains modest amounts of cobalt, but some growth zones in epigenetic pyrite are rich in cobalt. Cobalt- and copper-bearing fluids appear to have been generated during early diagenesis and to have migrated to sites of deposition in zones of soft-sediment deformation. These processes were probably promoted by submarine volcanism and sliding on the fan slope. The ore was deposited probably within 100 m of the seafloor, possibly due to rapid cooling or dilution of pore fluid by seawater.

Manuscript approved for publication November 30, 1988.

INTRODUCTION

A significant volume of cobaltiferous pyrite (Co-pyrite) occurs in metasedimentary rocks of the Middle Proterozoic Yellowjacket Formation at the No-Name deposit, in the area of Iron Creek, about 28 km southwest of Salmon (fig. 1). This is the southernmost known deposit of those constituting the Idaho cobalt belt (Hughes, 1983), all of which are stratabound in the Yellowjacket Formation. The No-Name Co-pyrite deposit differs in many ways from the larger deposits at the Blackbird mine 30 km to the north. Possibly the most important differences are the low arsenic content and simple sulfide mineralogy of the No-Name deposit, both of which are favorable for conventional smelting rather than requiring hydrometallurgical refining not currently (1987) available in the United States.

This study was undertaken as part of broader investigations of the geology and geochemistry of the Idaho cobalt belt by the U.S. Geological Survey under the Strategic and Critical Metals Program. A primary objective of the investigation of the Iron Creek deposits was to compare their geology and geochemistry with the better known cobalt deposits of the Blackbird mine area (Nash and Hahn, 1986). Goals of the projects were to describe the setting of the Co-pyrite deposits, controls on the distribution of cobalt, their geochemistry and mineralogy, and associated alteration, and to interpret conditions of formation and the potential for the occurrence of additional deposits.

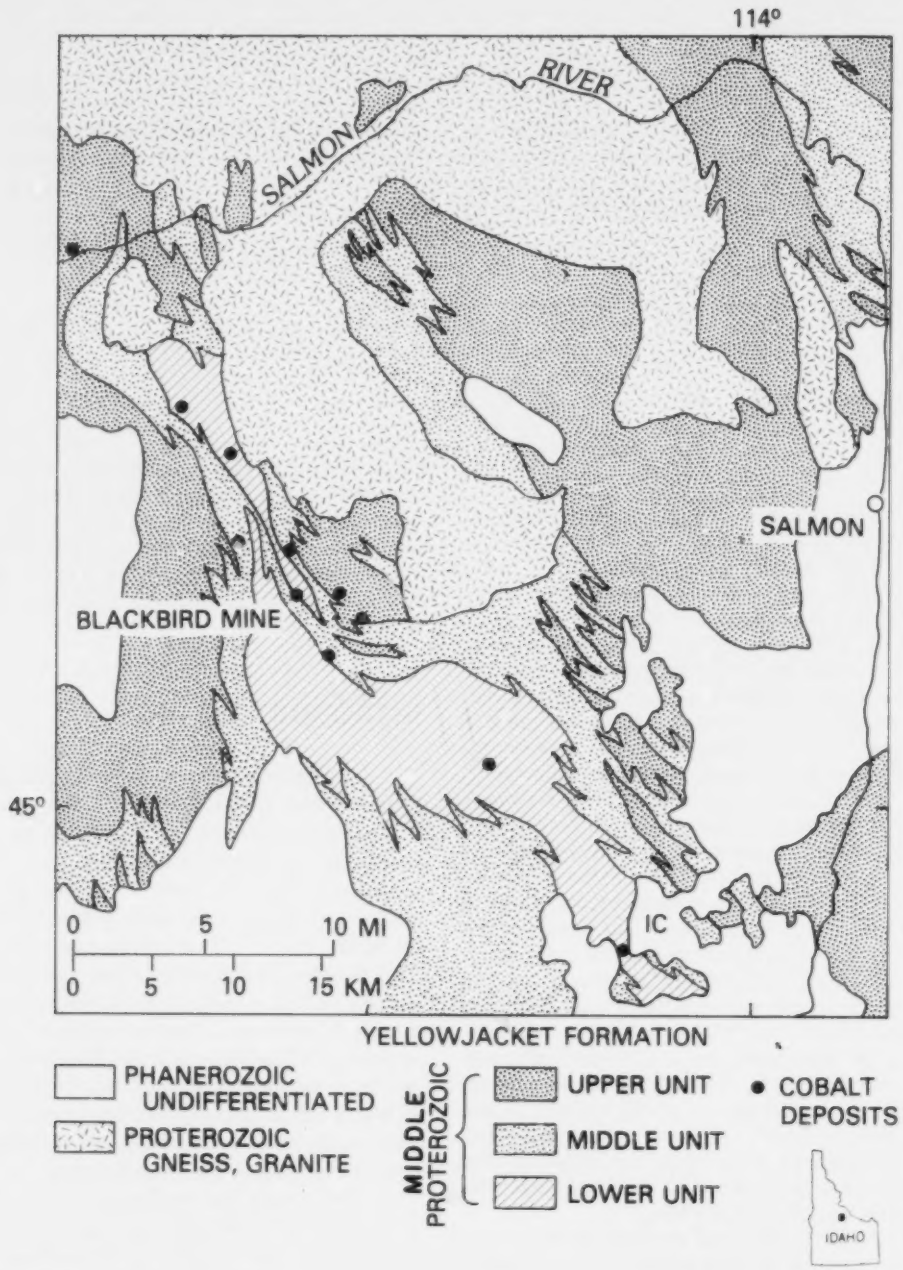

Figure 1. Location of Iron Creek area in Idaho cobalt belt, Lemhi County, Idaho. Generalized geology of region is from Hahn and Hughes (1984). Iron Creek deposits (IC) are at southeastern end of the cobalt belt.

This research was made possible by the cooperation of Noranda Exploration, Inc., who provided maps, geologic information, and access to drill core. Many Noranda geologists contributed important observations, in particular C.V. Chevillon, T.K. Stump, and T.A. Webster. I thank Vic Chevillon, Greg Hahn (formerly with Noranda Exploration, Inc.), and U.S. Geological Survey colleagues Jon Connor, Karl Evans, Dawn Madden, and Peter Modreski for helpful discussions.

PREVIOUS EXPLORATION AND GEOLOGIC STUDIES

The No-Name deposit was discovered during construction of a U.S. Forest Service road along the North Fork of Iron Creek in 1967 (Cohenour and others, 1973). From 1968 several claim owners and mining companies explored the area and discovered several zones of mineralization (fig. 2). The No-Name deposit, cut at the site of the present east adit, was recognized as containing abundant pyrite along with scattered chalcopyrite and secondary copper minerals as disseminations and fracture fillings in argillite and quartzite. Geologic, geochemical, and geophysical surveys preceded more than 5,700 m of diamond drilling and about 200 m of underground drifting from two adits. The east adit on the No-Name deposit encountered rock averaging 0.76 percent Cu and 0.19 percent Co, and drilling intersected as much as 142 m of rock mineralized with sulfides (in a 248-m hole), containing 0.99 percent Cu equivalent (Co percent = 4 × Cu percent; Cohenour and others, 1973). The average combined thickness of sulfide zones was about 50 m at an average grade of about 0.83 percent Cu equivalent. On the basis of geophysical, geologic, and drilling information in 1973, the No-Name deposit was estimated (Cohenour and others, 1973) to contain a resource of ". . . a few 100,000 tons to millions [of tons]."

Three other mineralized zones were identified in the Iron Creek area (Cohenour and others, 1973). (1) A zone rich in magnetite was found about 1.7 km southeast of, and parallel to, the No-Name zone (fig. 2). Called the "Jackass zone" for the canyon of that name, it seemed to contain only small amounts of copper and cobalt. The magnetite-pyrite deposit in the Jackass zone was apparently first discovered and staked in 1946; part of it is now well exposed in a roadcut of a logging road. (2) A zone of copper sulfate lies about 700 m north of the No-Name zone; geochemical and geologic studies prior to 1973 suggested this was a small, low-grade zone parallel to bedding and no further work has been done. (3) A zone of arsenopyrite containing traces of gold was found about 1.5 km north of the No-Name deposit and uncovered by a series of bulldozer trenches. The zone of veining is reported to be about 150 m wide, individual veins being as much as 2 m wide. The highest grade samples contained as much as 1 oz/ton Au, 0.4 percent Co, 0.4 percent Bi, and minor Ag (Cohenour and others, 1973).

Geophysics

The geophysical studies described by Cohenour and others (1973) are summarized here because that report is difficult to obtain. An induced-polarization (IP) survey in 1968 around the No-Name discovery cut suggested the presence of an east-trending zone of sulfide minerals ". . . several hundred feet wide and at least 1,700 feet long." All four holes drilled into this IP anomaly hit "significant sulfide mineralization." Subsequent "spontaneous polarization" measurements determined anomalies as large as 400 millivolts at sites of the strongest IP response. Additional IP lines run in 1971 enlarged the anomaly to about 240 m wide by at least 1,500 m long. Low resistivities were found in the IP anomaly.

Ground and airborne magnetic surveys detected the No-Name zone. A regional airborne survey (area 26 by 48 km, spacing 400 m, clearance 150 m) was made of the area as far north as the Blackbird mine. A linear magnetic high was detected over the Iron Creek area, but the Blackbird deposits produced no magnetic signature in the 1972 survey. The magnetic trend was interpreted to reflect a faulted, buried "magnetic igneous rock" (Cohenour and others, 1973). It is more likely that the magnetic high is caused by magnetite-rich zones in the Yellowjacket Formation. The east-trending magnetic anomaly is terminated at its eastern end by a structure interpreted by Cohenour and others (1973) to be a left-lateral fault. Ground magnetometer surveys determined an anomaly having "significant relief" only along a line across the middle of the No-Name zone. The author has found a magnetic susceptibility meter to be a useful tool for reliable detection of magnetic minerals in drill core and outcrop. Magnetic methods seem useful for detecting zones of magnetite in the Iron Creek area.

Geology

Early geologic studies were aimed at defining the geometry of the Co-pyrite zone and its metallurgical character (Cohenour and others, 1973). The IP anomaly previously described and 25 drill holes were used to define the No-Name zone as about 250 m wide and at least 1,500 m long. The early studies showed that the cobalt occurs in "lens-shaped bodies" interpreted by Cohenour and others (1973) to reflect ". . . zones of brecciation and bedding plane fractures, possibly related to bedding plane faults." Electron microprobe analyses showed that "cobalt occurs chiefly in the matrix (lattice) of pyrite crystals and that none occurs in the chalcopyrite. These results indicate that essentially no cobalt can be recovered with the copper and that to recover cobalt a separate pyrite concentrate will have to be produced" (Cohenour and others, 1973).

From 1977 to 1982, Noranda Exploration, Inc., undertook new studies of the Iron Creek area, focusing on the No-Name and Jackass zones. C.V. Chevillon, T.K.

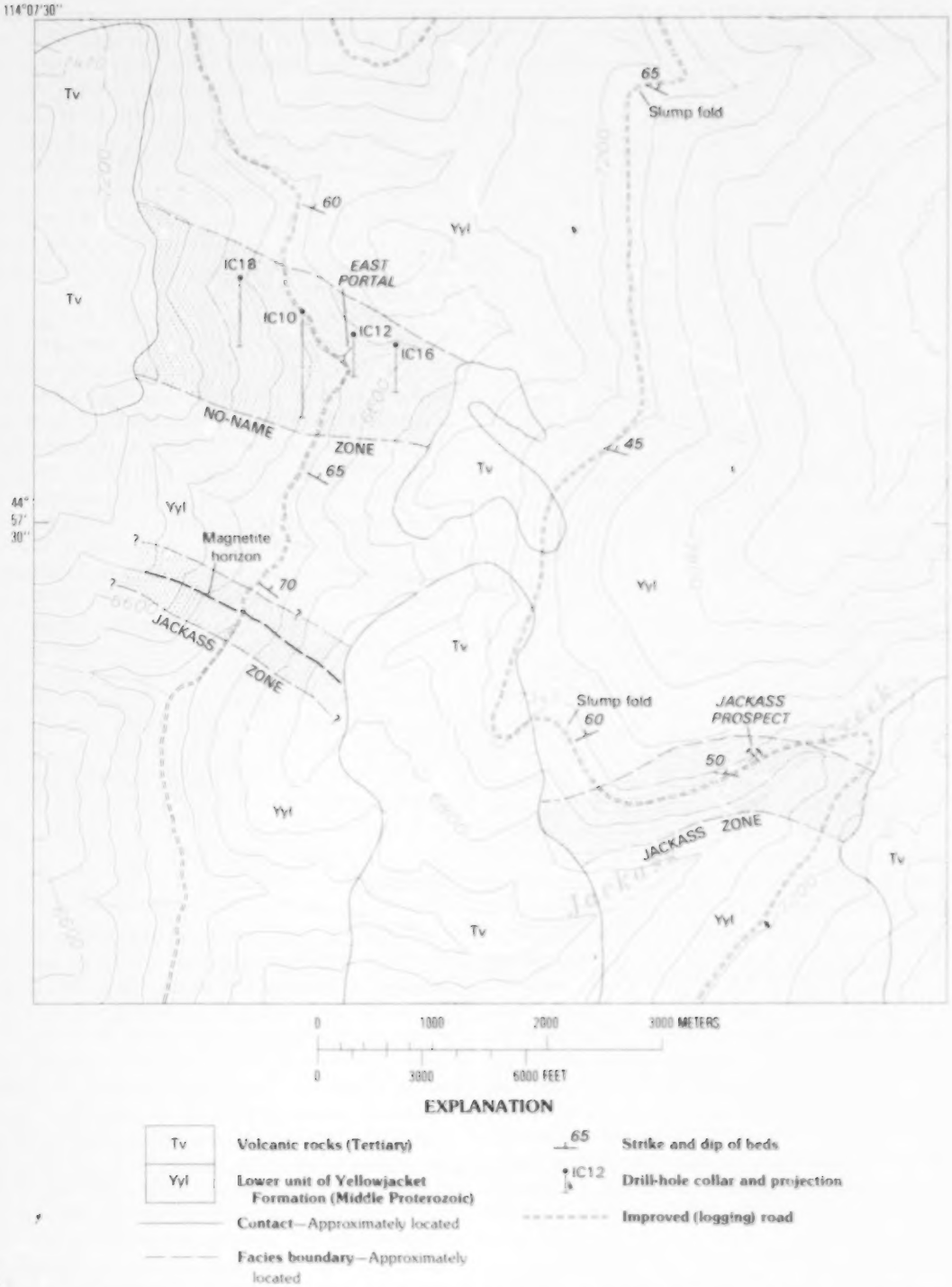

Figure 2. Generalized geology of Iron Creek area and location of Jackass and No-Name mineralized zones. Also shown are locations of drill holes sampled in this study. Geology generalized from Chevillon (1979). Base from U.S. Geological Survey, 1:24,000, Degan Mountain, 1962.

Stump, and T.A. Webster mapped the area in detail and relogged drill holes. Some of the work by Noranda at Iron Creek is alluded to by Hughes (1983), but important details remain hidden in unpublished maps and reports (Chevillon, 1979; Webster and Stump, 1980). The Noranda group traced several mineralized stratigraphic zones along strike for more than 1 km and recognized several types of soft-sediment deformation in those zones, including tight outcrop-scale folds and destruction of primary sedimentary textures. Noranda geologists recognized that the Co-pyrite is chiefly localized in zones of "fluidized" sediment that lack the fine lamination and many primary sedimentary structures of nearby Yellowjacket strata. They also documented the distribution of magnetite and pursued (without success) gold using the analogy of Tennant Creek, Australia: deposits similar to the No-Name prospect that are rich in magnetite, chlorite, and bismuth, as well as gold (Large, 1975).

Regional mapping and studies of ore deposits are reported by Modreski (1985), who provides an excellent framework for understanding the Iron Creek and other cobalt deposits. Modreski reports centimeter-scale polygonal cracks in the Yellowjacket that he interprets to have formed during periods of emergence.

GEOCHEMICAL METHODS

This study started in 1984 with examination of surface rocks at Iron Creek and logging and sampling of drill core. The locations of the drill holes are shown on figure 2. Approximately 200 slices of drill core a few centimeters long were taken for petrographic study. Samples for chemical analysis were of two types. Generally, if there was sufficient core, a one-quarter portion 20–50 cm long was sawn out. Some smaller samples were collected to focus on specific mineralized structures. Crushed core was used for places where the mineralized zones had been previously sampled more than once and for which very little core remained. The splits of crushed assay "reject" represent 2–5 ft (0.6–1.5 m) of core. Where possible, a slice representative of unmineralized or mineralized rock was cut from the analyzed material for petrographic study. Fifty-five samples were prepared as thin sections (most polished), and an equal number of slabs were polished. Brief descriptions of many of the samples are in Appendix 1. In this report samples are identified by the drill-hole number and depth in the hole (in feet), such as IC10–300.

Chemical analyses were made of 41 core samples; results are in table 1. Major elements were determined by X-ray fluorescence spectrometry (XRF), and minor and trace elements were determined by induction-coupled plasma spectrometry (ICP) and wet chemical methods. The analytical methods and their limits of detection are described in Appendix 2.

GEOLOGIC SETTING

Stratigraphy

The host rocks for the cobalt deposits are the oldest rocks in the area. These are fine-grained clastic rocks that have been metamorphosed to biotite grade of the greenschist facies. They probably are part of the Middle Proterozoic Yellowjacket Formation (Hughes, 1983). Another view (Modreski, 1985) is that these rocks are of Middle Proterozoic age but of uncertain correlation. Regional mapping reported by Hughes (1983) indicates that the Iron Creek rocks are part of the lower unit of the Yellowjacket (fig. 1). A similar correlation is proposed by Connor and Evans (oral commun., 1987) from their mapping in the Yellowjacket. The rocks in the Iron Creek area have a high proportion of argillite, possibly consistent with the interpretation of Hughes that the lower unit was deposited in a basin plain or fan fringe of a turbidite system but the small amount of graded bedding and other evidence for sedimentation from turbidity currents do not support such an interpretation. According to the reconstruction of Hughes (1983), the Iron Creek area was along the axis of a rift zone, possibly near a basin-margin fault. Paleocurrent measurements, chiefly on crossbedding and ripple crosslaminations, suggest sources on both the east and west margins of the rift basin (Hughes, 1983). Depositional conditions may have changed rapidly in the Iron Creek area. Local sand wedges suggest intermittent uplift or higher energy transport, whereas sequences of dark argillite suggest quiescence in a starved-basin stage (Hughes, 1983). Argillite containing abundant laminated fine-grained pyrite in the Iron Creek area supports the starved-basin stage. Bedded iron-formation at several localities in the Jackass Creek and No-Name areas suggests quiescence, the unusual concentrations of iron coming from seafloor vents. There are no red rocks in the Iron Creek area that might suggest oxidizing intertidal conditions, but mud-chip conglomerate and sand-filled polygonal structures found in the Yellowjacket about 10 km northeast of Iron Creek (Modreski, 1985) seem to be restricted to areas of strong currents, possibly shallow water and emergence. However, most of the evidence suggests that the lower part of the Yellowjacket was deposited below wave base. About 300 m upsection (west) from the No-Name mine, sandier beds are more widespread and mark the approximate base of the middle unit of the Yellowjacket (Connor, oral commun., 1987).

Mafic igneous rocks are present in the area and seen in float, drill core, and rare outcrops. They are presumed to be of Proterozoic age because they are metamorphosed to the same grade as the Yellowjacket. Some mafic rocks retain a porphyritic fabric, but all are altered and metamorphosed. Details of their geometry and composition are not well known. In drill core the igneous rocks have massive fabric for a meter or more, which suggests they are intrusive. An outcrop near the Jackass prospect was interpreted as a bedded pyroclastic rock by R.L. Earhart (oral commun., 1986). Both mafic dikes and coeval pyroclastic rocks may be present, as they are in the Blackbird mine area (Hahn and Hughes, 1984), but they are not abundant in the Iron Creek area.

Tertiary volcanic rocks of the Challis volcanic field cap ridges in the area. These rocks were deposited on a surface having considerable relief. The Tertiary rocks are not known to be involved in processes forming or modifying the cobalt deposits, but they cover the south end of the No-Name zone.

Structure

Yellowjacket strata in the Iron Creek area generally dip about 50°–75° to the northwest or northeast (fig. 2). Several north-striking faults cut Tertiary volcanic rocks, but faults are difficult to recognize in the Yellowjacket. Cohenour and others (1973) describe geophysical anomalies that they interpret to reflect faults, but these have not been confirmed on the ground. Local changes in dip suggest the presence of several broad folds in the Jackass Creek area (Chevillon, 1979), and some outcrop-scale folds are interpreted to be slump folds (Webster and Stump, 1980). In 1987 C.V. Chevillon showed me some of the tight folds, and I would agree that they seem to be soft-sediment rather than tectonic structures. Bedding in these folds is highly contorted, and the axial region of the folds is filled by material that resembles liquefied sand in a sandstone dike; there is very weak axial-plane cleavage. In the No-Name zone, strata consistently dip about 60° NW. and no major faults or folds have been recognized in drill core or outcrops.

Cobalt deposits in the Iron Creek area are stratabound, and locally stratiform, but a major proportion of the ore minerals occurs within synsedimentary soft-sediment structures (fig. 3). These discordant structures, which will be described in a later section, produce lumpy to massive fabric (fig. 4*B*–4*G*) with few of the finely laminated beds that are typical of the Yellowjacket. Although the genesis of these fabrics is open to debate, the disruption structures and retextured fabrics are distinctive and diagnostic features of these mineralized zones. In drill core or good outcrop one can see a progression over tens of meters from beds having excellent lamination at millimeter scale to strata having no primary bedding features. Well-developed primary and secondary sedimentary structures are so widespread and typical of the Yellowjacket (Hughes, 1983; fig. 5*A*, this report) that their absence is noteworthy and is presumed to reflect destruction or retexturing following sedimentation. Zones that lack characteristic primary and secondary sedimentary structures are generally above beds that display abundant evidence for dewatering: sand dikelets, load casts, and wispy bedding. Noranda recognized the destruction of these sedimentary features in 1978 and called such beds "fluidized" in reference to the process believed to have caused the destruction of features. The nongenetic term "disruption" will be used in this report to describe beds that have partly or completely lost their primary bedding characteristics. Because cobalt deposits are localized in disruption structures and appear to have formed together, these structures will be discussed further in later sections.

JACKASS ZONE

The Jackass zone, about 300 m stratigraphically below the No-Name zone, contains abundant magnetite and pyrite in a 10-m-thick section of conspicuously orange-brown argillite and siltite that crops out in the upper part of Jackass Creek, about 1.7 km northeast of the No-Name adit (fig. 2). This gossan was staked in 1946, later was deeply cut for a logging road, and now is called the "Jackass prospect." The zone of magnetic minerals has been traced on strike for several kilometers (Webster and Stump, 1980) and crops out 700 m east of the No-Name adit on the Iron Creek road. The roadcut through the Jackass prospect exposes about 5 m of metasedimentary rock containing abundant magnetite or magnetite and pyrite, now highly oxidized. Some of the magnetite is layered and could be called banded iron-formation (BIF), but most of it has massive, swirled, or veinlike fabric. Some of the exposed ferruginous metasedimentary rock is moundlike in form, about 1 m high and 2–4 m wide. The exposures along the Iron Creek road contain thinner zones of magnetite and very little pyrite; the magnetite is partly bedded and partly in lumps, swirls, or thin crosscutting stringers. Much of the magnetite in the Jackass zone is inconspicuous in the dark argillite and siltite, but is easily detected with a magnetic-susceptibility meter. Concentrations of 1 percent are common, and some parts contain more than 50 percent magnetite across beds or structures 10–20 cm thick. Some pods or disruption features in the magnetite-bearing strata contain tourmaline that possibly is genetically similar to the tourmaline that cements breccia

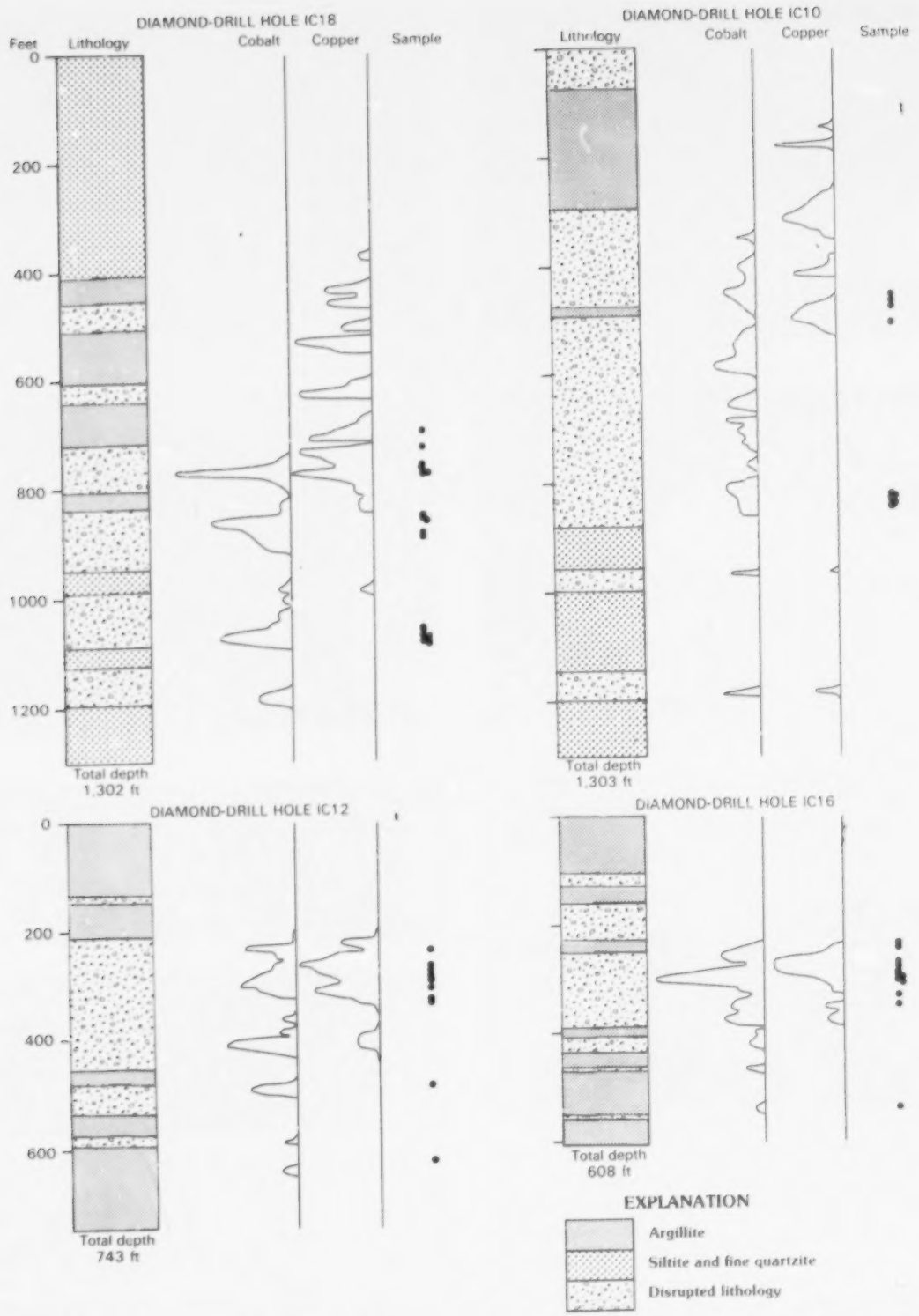

Figure 3. Generalized lithologic logs of drill holes through the No-Name deposit in the Yellowjacket Formation showing distribution of disruption zones, cobalt, and copper. Drill-hole locations shown on figure 2. Copper and cobalt values are generalized from assays by Coastal Mining Company.

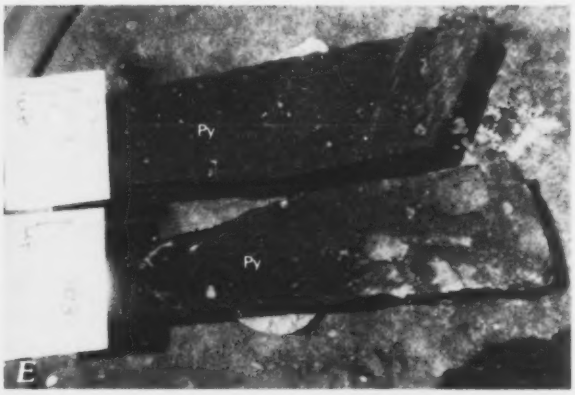

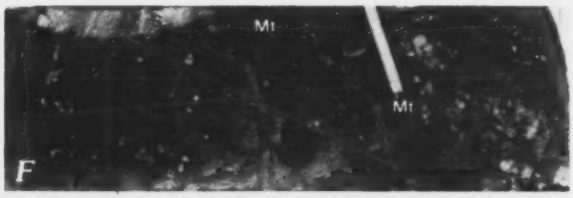

north of Iron Creek and especially near the Blackbird mine (Modreski, 1985; Nash and Hahn, 1986).

The Jackass zone strikes about N. 80° W., and the zones of magnetite±pyrite are generally conformable with enclosing unmineralized strata. However, in detail the magnetite-bearing strata show evidence for soft-sediment deformation that includes loss of primary bedding structures and redistribution in local dikelike features. These soft-sediment features resemble those in the No-Name zone, discussed in more detail in the next section. Siltite and fine quartzite about 100 m stratigraphically above the Jackass zone are involved in several outcrop-scale slump folds that possibly reflect the same general conditions of sediment instability as are evident in the Jackass zone.

Gossan developed in areas of iron mineralization in the Jackass zone locally contains patches of pink or green minerals, suggesting the presence of some cobalt or

Figure 4 (facing page). Drill core from the Yellowjacket Formation showing disruption structures. All drill core is 4.5 cm wide. *A*, Contrast in bedding character: two cores on right show typical good lamination of argillite and siltite, whereas two cores on left show disrupted bedding. Disruptions contain clasts of sediment similar to enclosing strata; epigenetic quartz and pyrite cement disruption fill. Some disruptions are aligned parallel to enclosing strata and others are discordant (IC10, 260- and 300-ft intercepts). *B*, Sawn drill core in disruption zone showing lump breccia, massive pyrite (Py), and discordant veinlike structures, some of which contain magnetite (Mt) (IC 18, interval approximately 1,069- to 1,088-ft depth). *C*, Disruption zone showing clasts of siltite (S), magnetite (Mt), and injected clay (I) (IC10, parts of interval 809- to 827-ft depth). *D*, Clasts of siltite in disruption zone having rounded edges cemented by clay (I) that seems to have been injected between fragments (IC10–824). *E*, Two zones of very rich massive-textured pyrite about 15 cm thick that fill disruption structures; hangingwall is bedded argillite. Clasts of siltite float in pyritic matrix (IC10, 303- and 304-ft depth). *F*, Subround clasts of magnetite (Mt) and siltite (S) in disruption zone; polished slab of drill core (IC18–1090). *G*, Layer of fine-grained pyrite "mud" (Py, upper half of slabbed core) that is partly bedded and partly deformed (ragged interface with siliciclastic material); siltite (S) has lumpy breccia texture (IC12–305).

copper in secondary minerals. However, assays of numerous rock-chip samples and core from two diamond drill holes reveal that only a few localities contain as much as 1,000 ppm Co (Webster and Stump, 1980). Current information suggests that the magnetite-rich parts of the Jackass zone are too thin and contain too little cobalt and copper to be a significant resource. However, these iron-rich deposits are an important geochemical feature of the Idaho cobalt belt and the evolving Yellowjacket basin. Many visitors to the Jackass prospect comment on the probable similarity of these deposits to ferruginous deposits formed on the seafloor by "black smokers" (for example, Mottl, 1983).

THE NO-NAME DEPOSIT

Structure

Strata in the No-Name deposit have consistent dip where bedding is evident. No local abrupt changes in attitude are seen, such as would be expected at the hinge of a fold. Layering of ore minerals is generally parallel to layering of siliciclastic components, both in fine-grained layers thought to be clastic and in layers of coarse-grained minerals thought to be the result of epigenetic processes. Faults are neither evident in drill core nor required to explain any features, but bedding-plane slip is possibly indicated by smearing of layers parallel to bedding (fig. 4*D*, 4*E*).

The most conspicuous structural feature of the No-Name deposit is zones that lack primary sedimentary textures (fig. 3). Generalized at deposit scale (fig. 3), these zones contain numerous centimeter-scale disruption structures that are mostly discordant, although some are concordant with bedding (where present). Some of the disruption structures are filled by veinlike material that is coarse grained and rich in pyrite, but the margins of the structures are not sharp like hard-rock veins and characteristically the enclosing rocks have lump-breccia[1] textures believed to indicate formation from incompletely lithified sediment.

Significant cobalt intercepts (>0.1 percent) are in every case in zones of disrupted bedding, as shown schematically on figure 3. Intervals of bedded fine pyrite or magnetite contain little cobalt, whereas intervals of discordant structures filled by pyrite, generally of coarser grain size, contain notable amounts of cobalt. The disruption structures are important at two scales: At bed, or centimeter, scale it is clear that Co-pyrite is confined to the disruption structures. Good examples are the thin zones 1–10 cm thick, containing abundant coarse pyrite, that produce cobalt "kicks" greater than about 0.3 percent for a 0.3- to 0.6-m interval of core. At deposit scale, the Co-pyrite zones of minable proportions are within a zone of numerous disruptions that is considerably thicker than the cobalt zone. For example, drill hole 10 encountered numerous disruptions over an interval of nearly 200 m. Within this interval the amount of disruption is highly variable: some parts consist of good bedding typical of the Yellowjacket, whereas in other parts almost no bedding can be recognized in the swirled mass. Not all disrupted zones (at centimeter scale) contain significant Co-pyrite, but Co-pyrite exists only in disruptions. Stratiform fine-pyrite layers contain as much as 3,600 parts per million (ppm) Co, but generally are too thin at this grade to constitute a significant contribution of cobalt.

Lithology

Yellowjacket strata in the Iron Creek area are generally very fine grained and rich in micas. Argillite and siltite beds a few millimeters to 1 cm thick are most typical, and the strata include lesser amounts of fine-grained quartzite. The rocks are generally medium gray green to charcoal gray on unweathered surfaces and tend to be lighter in weathered zones. Limonitic coatings are abundant in two gossan zones. Sedimentary features are conspicuous in drill core (fig. 4*A*) and in many large outcrops along Iron Creek.

[1]Term used for description only; no analogy to the "lumps" in carbonate rocks is implied.

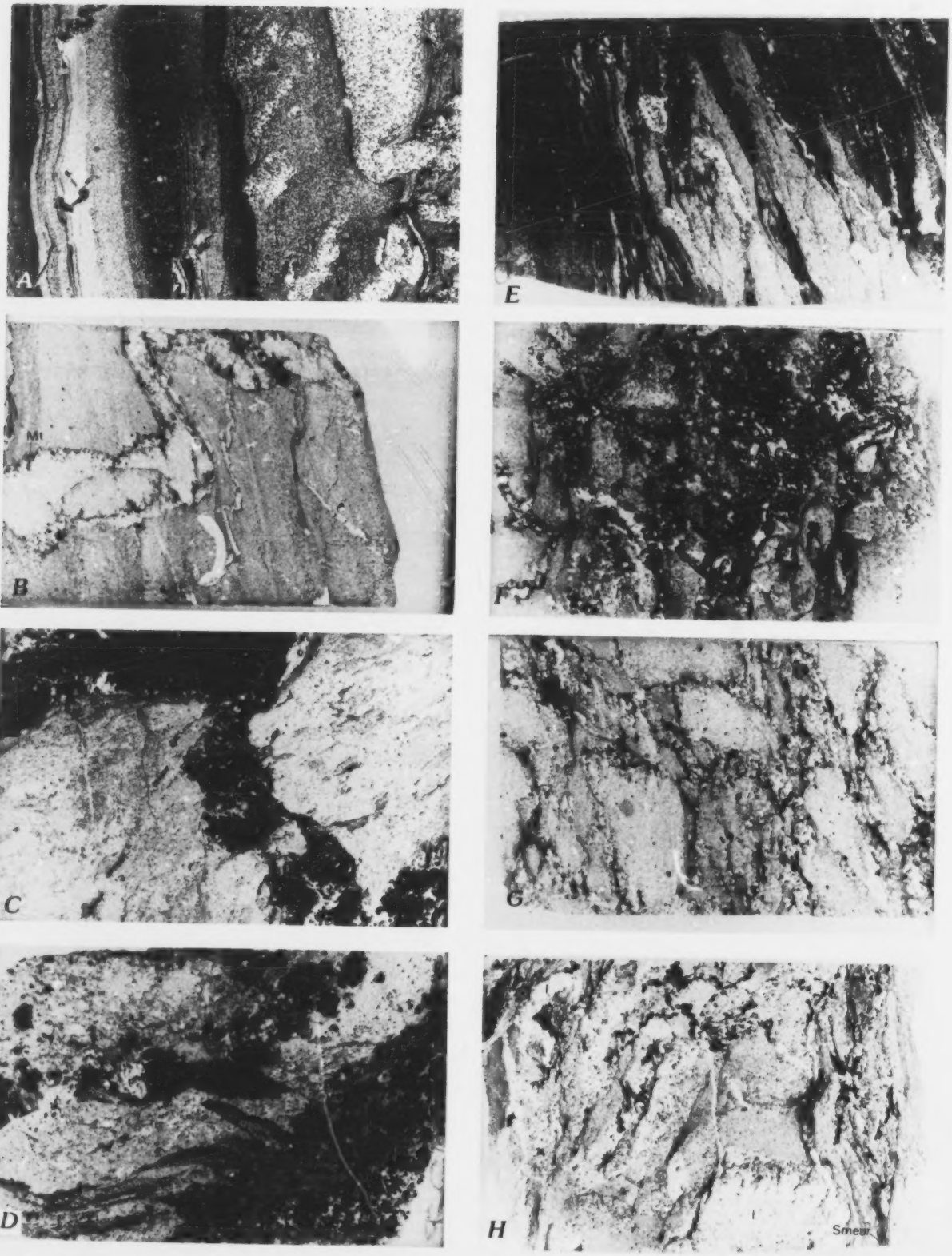
A
E
Mt
B
F
C
G
D
H
Smear

The No-Name deposit occurs within a sequence of argillite and siltite about 500 m thick that is distinct from underlying and overlying Yellowjacket strata, which are somewhat coarser grained and have better bedding features. Those footwall and hanging wall strata are micaceous fine quartzite. The No-Name zone contains very little quartzite. The general lack of bedding and other sedimentary structures in these fine-grained rocks is unusual for the Yellowjacket Formation. Close inspection of excellent outcrops, drill core, and thin sections indicates that the bedding features typical of the Yellowjacket (fig. 4*A*, 5*A*), both regionally and nearby in Iron Creek canyon, were destroyed over scales of 1 cm to several meters prior to complete consolidation.

Proportions of quartz, white mica, biotite, chlorite, and feldspar vary from bed to bed. The argillite contains more white mica than it does biotite, and generally the white mica is very fine grained (< 25 μm; fig. 6*B*, 6*E*). Some biotite is fine grained, about 30–50 μm, but much is 100 μm or more and occurs in association with "veinlike" quartz of similar grain size (fig. 6*D*, 6*E*). The "veinlike" quartz is totally intergrown, has no rounded clastic form, and is coarser than in quartzite beds. White mica intergrown with the "veinlike" quartz also is coarse grained (75–200 μm; fig. 6*C*) and could be termed muscovite. Erratic swaths of coarse quartz, biotite, and white mica in finer siltite or argillite (disruption structures) do not have the sharp walls of true veins. Plagioclase feldspar constitutes as much as 10 percent of some thin sandy layers.

Ore minerals of the No Name deposit are present in four lithologic contexts: (1) Very fine grained pyrite, generally in clearly defined laminae, is interbedded with argillite and to a lesser extent with siltite (fig. 6*A*, 6*E*). (2) Coarse-grained pyrite is intergrown with the fine pyrite along bedding or within discordant disruption structures (fig. 6*F*, 6*H*). (3) Chalcopyrite fills crosscutting stringers and surrounds coarse pyrite in disruption structures. (4) Magnetite occurs as fine grains that are bedded or in discordant veins, with or without pyrite (fig. 4*B*, 4*F*). Where magnetite is abundant (>30 percent), it generally is in rounded or lumpy aggregates (fig. 4*F*, 5*C*). Only rarely do the ore minerals fill structures having sharp margins typical of veins; rather, they occur in much the same setting as terrigenous clastic grains and recrystallized derivatives.

Figure 5 (facing page). Thin sections showing textures of sedimentary rocks from the Yellowjacket Formation. All about 4 cm wide and photographed in transmitted light. *A*, Well-laminated sample of Yellowjacket Formation from near Blackbird mine showing well-preserved sedimentary features such as graded bedding, sand dikelets, and compaction features; these features are rarely seen in strata of No-Name zone. *B*, Siltite showing weakly developed lamination, cut by sand dikelet that was folded during compaction; dark specks on margin of sand dikelet are grains of magnetite (Mt) (IC18–474). *C*, Magnetite (opaque) in wisps and sinuous injections in siltite (IC10–821). *D*, Siltite containing discontinuous microlenses of fine pyrite "mud" (truncated by bedding plane slip?), cut by injection structure containing abundant coarse pyrite (IC18–445). *E*, Siltite containing truncated beds of pyrite "mud" (opaque) and thin clasts of argillite; this texture seems to be caused by low-angle slip structures subparallel to bedding (IC12–305). *F*, Lump breccia of small pieces of argillite and siltite, cemented by quartz and pyrite; most clasts have round edges, but some are angular (IC12–323). *G*, Lump breccia of argillite and siltite clasts; the embayments in some clasts suggest some plastic deformation (IC10–829). *H*, Complex disruption texture that is a combination of tabular clasts, smear, and sand injection (I) (IC10–731).

Soft-Sediment Deformation

A great variety of complex small structures are seen in drill core (fig. 4) and in some exceptional outcrops. These structures are discordant and have a variety of surfaces: curved to angular, sharp to gradational. Strata in and near the structures commonly contain rounded or bent fragments or have massive to swirled fabric. The structures and the unusual clastic fabrics are believed to have formed prior to consolidation. Nomenclature of these features is a problem: experts on the subject (for example, Elliott, 1965; Lowe, 1975) do not seem to agree on terminology, much of which is genetic rather than descriptive. However, sedimentologists and soil scientists agree that (1) disruption of unconsolidated sediment is most likely in rapidly deposited sequences of clay, silt, and fine sand that have porosities of about 50 percent; and (2) cohesion is lowest for silt- and fine-sand-size grains.

The following descriptions are based chiefly on drill core that does not permit determination of the strike of structures and bedding. Also, core provides excellent exposure of small features but no information about the rocks a few centimeters away. In the core that I inspected from five drill holes, the dip of bedding (where present) was remarkably consistent across tens or hundreds of meters. The following types of structures were observed, and seem to be distinct, although in many exposures several structures seemed to be combined.

Contorted beds.—Bent, swirled, or erratic layering at scales from a few millimeters to several centimeters is common. Some features resemble convolute bedding. Most are probably developed in clay or silt beds by loading, but in the No-Name zone associated features suggest loss of cohesion. These structures are not folds such as seen in some clastic rocks that were deformed during diagenesis (for example, Jonasson and Goodfellow, 1986); indeed, small, centimeter-scale folds are rare in the No-Name zone.

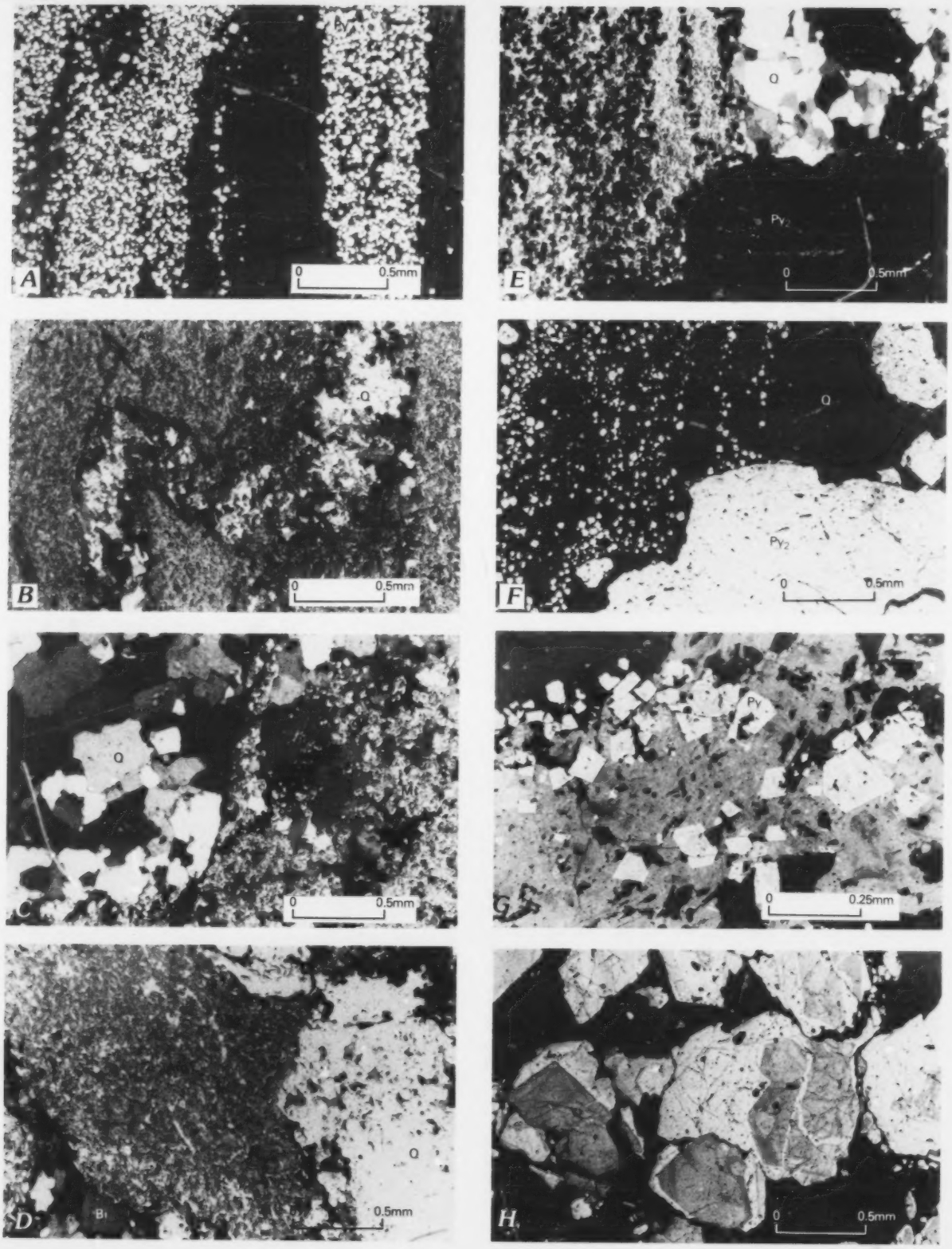
A
Py
0
0.5mm
E
Q
Py2
0
0.5mm
B
Q
0
0.5mm
F
Q
Py2
0
0.5mm
C
Q
0
0.5mm
G
Py
0
0.25mm
D
Q
Bi
0.5mm
H
0
0.5mm

Injection structures.—These are crosscutting structures generally less than 1 cm wide that contain chiefly sand-sized quartz, with or without pyrite or magnetite (fig. 4*D*, 4*E*, 5*B*, 5*D*). In thin section the quartz is coarser than is characteristic of adjacent sandy beds and is suspected to represent quartz cement added around sand grains. Micas are not abundant. Where these structures cut beds they are clearly visible, but texturally similar fabrics having concordant contacts might reflect injection parallel to bedding or possibly liquefied or fluidized beds (described following). Where the crosscutting material is rich in clay, injection in a viscous or plastic state seems possible (fig. 4*D*).

Massive fabrics.—Rocks showing little or no internal fabric are common and clear exceptions to the normally well bedded or laminated Yellowjacket strata. Many of these examples seem to be contained within undisturbed argillite or quartzite beds, although in some the enclosing rock has a lump-breccia texture (see following). Much of the rich magnetite or coarse-grained Co-pyrite occurs in 2- to 10-cm swaths having this massive fabric (fig. 4*C*, 4*E*).

Lump-breccia texture.—Rounded fragments of quartzite, siltite, or argillite are common in disrupted zones (fig. 4, 5). The lumps are generally 0.5–2 cm in diameter and rarely are angular (fig. 5*F*, 5*G*, 5*H*). Lump breccia generally is present adjacent to vein-like discordant structures. Fragments of argillite are tabular and commonly are bent. Very similar textures are described as "pelletoid conglomerate" by McNeil (1966).

A variant of lump breccia has crudely aligned fragments and a gneissic fabric (fig. 5*H*); these are mostly dark-colored rocks that are not photogenic. The clasts are generally aligned with the plane of bedding in enclosing strata. This fabric seems to reflect shear or bedding-plane slip during or after brecciation, as might happen during slumping or sliding.

Lenticular fabric.—This fabric is characterized by microlenses a few millimeters thick and less than about 3 cm wide that have feathery ends (fig. 5*D*, 5*E*). The lenticular features are most easily seen in very fine pyrite or clay, possibly because they have high color contrast, and seem to be produced by shear or slip parallel or subparallel to bedding.

Many of the secondary fabrics seem consistent with formation during downslope sliding of partly or completely liquefied sediment. The prevalent disturbed bedding, both within the No-Name deposit and elsewhere in the Yellowjacket, is commonly developed in interbedded clay, silt, and fine-sand sequences (see, for example, Lowe, 1975) and generally attributed to plastic deformation due to loading. The crosscutting sand dikelets also are commonly developed in such sequences and are attributed to liquefaction or fluidization by pore fluids and upward transport. My impression of the No-Name zone is that vertical features related to dewatering are less common than subhorizontal features confined between beds. Also, retextured clean sandstone or quartzite is rare; thus, winnowing of clays seems to have been uncommon in the No-Name zone, suggesting that fluid velocities were generally not high, or in the range characteristic of fluidization (Swarbrick, 1968; Lowe, 1975). The majority of features tend to be aligned parallel to bedding and involve a high proportion of grains and clasts, similar to features in "slurry-slumps" and "slide-slumps" described by Elliott (1965), although documentation of horizontal displacement is difficult in drill core. Fluidized injections can form between beds (Lowe, 1975; Hiscott, 1979), but this does not seem to be as common elsewhere as more vertical geometries. At Iron Creek the parallelism of features with bedding seems more consistent with liquefaction—the ". . . sudden loss of shearing resistance associated with grain framework collapse and a rapid but temporary increase in pore fluid pressure" (Lowe, 1975, p. 159). Sedimentologists note that liquefaction of unconsolidated sediment can cause mass movement on very gentle slopes (less than 10°) that in some ways resembles transport by turbidity currents, but does not produce graded bedding (Middleton and Hampton, 1973). The association of clastic dikes with slump folds has been noted (Dzulynski and Randomski, 1956; Hiscott, 1979) and demonstrated to occur at less than 60 m of burial.

Figure 6 (facing page). Photomicrographs of textures in thin sections of samples from the Yellowjacket Formation. Q, quartz; Py, pyrite. *A*, Layers of fine pyrite "mud" (white cubes; Py) interbedded with clay (now argillite); reflected light (IC12–305). *B*, Sand dikelet in argillite (Arg); fold probably was produced by compaction of original clay-rich sediment. Quartz grains are about 200 μm, coarser than in adjacent beds, probably explained by diagenetic grain growth; transmitted light, crossed polarizers (IC18–474). *C*, Quartz and mica (Mi) filling disruption structure; the quartz grains are larger than clastic sand grains in adjacent beds, and the mica (muscovite) is also much coarser than in beds—both types seem to reflect diagenetic growth; transmitted light, crossed polarizers (IC10–460). *D*, Clast of clay (Arg) in disruption structure that seems to have been squeezed into veinlike filling of coarse quartz (Q). Quartz and coarse flakes of biotite (Bi) cement clasts; transmitted light, crossed polarizers. *E*, Layered fine-grained pyrite "mud" in argillite, abutted by coarse grain of pyrite (Py_2) in quartz-rich disruption; transmitted light, crossed polarizers (IC16–300). *F*, Same field as E, showing differences between early bedded pyrite and later coarse pyrite (Py_2) in disruption; reflected light (IC16–300). *G*, Euhedral, zoned pyrite engulfed by massive pyrite; reflected light (IC12–323). *H*, Coarse-grained pyrite in which growth zones are revealed by tarnish. Dark zones are purple to blue, presumably reflecting an impurity in the pyrite lattice. This tarnish develops after several months of exposure to atmosphere; reflected light (IC18–861).

Ore Mineralogy

The No-Name deposit contains a limited suite of ore minerals. Pyrite, magnetite, and chalcopyrite are the common ore minerals, along with traces of marcasite, hematite, and various copper oxide minerals.

Pyrite occurs in four forms: fine-grained, coarse-grained, anhedral, and corroded. Fine-grained pyrite, less than about 50 μm in grain diameter, tends to be laminated and most abundant in argillite. The texture and association with argillite suggest that this was a syngenetic iron sulfide mud; recrystallization during diagenesis and metamorphism is likely, but does not seem to have produced many changes. Coarse-grained pyrite occurs both within laminae of fine pyrite, in which it probably is a recrystallization product, and in discordant structures. All of this pyrite takes a good polish, shows no replacement relations with other ore minerals, and is free of internal structures other than growth zones that tarnish to various shades of orange or purple (fig. 6*G*, 6*H*). Coarse pyrite probably is slightly more abundant than is fine. Anhedral pyrite that formed late in the paragenesis surrounds other sulfide grains (fig. 6*G*). This variety tarnishes to shades of purple and blue and has no crystal form, although some grains seem to have cleavage. According to scanning electron microscope–energy dispersive system (SEM–EDS) analysis, the general composition is the same as pyrite, but minor elements below about 1 weight percent could not be determined. It is optically isotropic and thus is tentatively identified as pyrite; the unusual morphology may be inherited by replacement of an earlier mineral. A minor variety of pyrite is characterized by porous texture and corroded outlines; this may have originally been pyrrhotite, as at the Blackbird mine, but lacks the concentric banding of that sulfide (Nash and Hahn, 1986). Some of this corroded iron sulfide is marcasite.

Magnetite occurs in trace to major amounts as well-formed crystals about 10–200 μm in diameter. It is generally euhedral, and no lamellae of ilmenite or other minerals have been seen. Microprobe analysis (Modreski, 1985) showed less than 0.02 percent TiO_2 and very low cobalt. There is no evidence to suggest that any of the magnetite grains are detrital. The magnetite was an essential part of the sediment from early in its history, like pyrite and quartz. Some is clearly bedded, a chemical sediment, and some is in disruption structures. Some very interesting occurrences are in sand dikelets, where the magnetite occurs along the margins of the dikelet (fig. 4*B*). The magnetite in discordant structures possibly was introduced in part as solid particles, along with quartz sand grains, but most grains are too large to have been in hydraulic equilibrium with silicates and thus are presumed to have grown larger in place.

Chalcopyrite is a common mineral but rarely is as abundant as pyrite. It fills the matrix around pyrite crystals and tends to be most abundant in the upper part of cobalt zones (fig. 3). The paragenetic and spatial position of chalcopyrite suggests it formed late in mineralization. Films of oxidized copper minerals coat chalcopyrite in zones near the surface.

Cobalt appears to reside in pyrite rather than in a distinct cobalt mineral, such as in cobaltite in the Blackbird deposits. My petrographic studies have found no cobalt-rich minerals in even the richest cobalt zones, those assaying greater than 1 percent Co. Coastal (Hanna) Mining Company and Noranda Mining Company found no cobalt minerals but determined 2.5–4.5 percent Co by microprobe analyses in one variety of pyrite, and they concluded that cobalt is in the pyrite lattice (Webster and Stump, 1980). Modreski (1985) found 2–3 percent Co in pyrite. Reasons for the wide variation in cobalt content of the pyrite have not been established, but presumably relate to the times and conditions of pyrite growth.

Arsenic is notably less abundant in the No-Name deposit than in the Blackbird ores, and no arsenic-rich minerals have been identified to date. Some preliminary microprobe analyses by Noranda Mining Company (Webster and Stump, 1980) indicate that 0.3–0.8 percent As is present in some pyrite growth zones. Incorporation of a few percent of cobalt or arsenic in the pyrite lattice, although not common, has been reported and accepted for other sulfide deposits (Ramdohr, 1980).

Alteration

Alteration of the host rocks in the No-Name deposit is subtle and possibly obscured by later regional metamorphism. Three types of alteration are developed in and near the Co-pyrite deposits: (1) Most typical and widespread is potassic alteration in which potassium micas were developed or remained stable. One example is the association of coarse white mica (muscovite) with coarse quartz and pyrite in disruption structures (fig. 6*C*). Coarse biotite in association with muscovite, pyrite, and quartz is also probably an early-formed phase rather than a metamorphic product. High silica activities are suggested for the potassic alteration on the basis of strong silica cementation and formation of coarse grains of veinlike quartz. No selvages of micas or other minerals are noted around the disruption structures, their absence indicating that the fluid in the structures was in equilibrium with the surrounding sediment. (2) Formation of carbonate minerals is notable in many pyritic disruptions. Tan carbonate (ankerite?) cements the disruption fill and locally replaces biotite and pyrite. Similar iron carbonate cements some disruption struc-

tures in the Blackbird mine area (Nash and Hahn, 1986). (3) Tourmaline cements breccia and disruption zones near the No-Name deposit, in many places in association with magnetite. Tourmaline is present as a minor accessory mineral in some parts of the No-Name deposit and reflects introduced boron rather than clastic grains, but it is not abundant or obviously related to formation of Co-pyrite. These three types of alteration are compositionally distinctive and are evident despite metamorphism that probably caused recrystallization of the minerals associated with ore.

Bright green chlorite showing anomalous blue birefringence is developed in and near many sulfide layers. This chlorite replaces brown biotite and especially favors the coarser grains of biotite in disruption structures. The texture of the chlorite indicates it is a post-metamorphic feature, a retrograde product not related to ore formation.

Alteration associated with pyrite zones is not a simple guide to ore because the chemical and mineralogical changes are minor and not easily seen. Color of metamorphic rocks does not seem to be significantly different in zones of alteration associated with ore; the brighter shades of green in some zones seem to reflect retrograde alteration. Also, the altered rock is mostly concordant with bedding at deposit scale and is not as easily seen as discordant alteration along faults or veins.

GEOCHEMISTRY

Results of chemical analysis for major and minor elements are shown in table 1 and summarized in table 2. Major-element concentrations are typical of fine-grained metasedimentary rocks except for the unusually high concentrations of iron and sulfur in samples containing sulfides or magnetite. Considering the high to extremely high concentrations of iron, there is relatively little manganese. Mineralized samples contain as much as 10,000 ppm (1 percent) Co and Cu, and some samples are slightly enriched in Ag, As, Au, Bi, Cr, Mo, Pb, and Zn (table 2). A comparison of mineralized and barren footwall or hanging wall samples (table 2) using discriminant function analysis (Davis, 1986) indicates that Fe, S, As, Ba, Bi, Co, Cr, Cu, Ni, Pb, Se, and Zn are significantly higher in Co-pyrite zones. These pyrite zones are slightly depleted in Al, Na, K, and Ti. Concentrations of most minor elements in mineralized samples are not significantly different from those in barren samples.

The geochemistry of the cobalt-enriched zones is dominated by associations with sulfur as sulfide. Correlation analysis (Davis, 1986) and scatterplots (fig. 7*A*) indicate a direct and invariable association of cobalt and total sulfur. Cobalt is strongly associated with Fe, As, Se, Ni, Pb, and Bi and less so with Cu (fig. 7*D*). Some cobalt zones have notably low concentrations of Cu (<20 ppm), such as in footwall strata containing magnetite. Correlation coefficients of cobalt with most rock-forming elements such as Mg, Ca, K, and Na are weakly negative, indicating that Co-pyrite is not associated with any unusual mineral assemblage other than with sulfides.

The general composition of the mineralized samples from the No-Name deposit is similar to ores from the Blackbird district in several aspects and different in others. The mineralized rock is similar in its high concentrations of Fe and some other "mafic" elements such as Bi, Cr, and Ni and notably low concentrations of Ag, Pb, and Zn compared to many sediment-hosted base-metal deposits. The No-Name deposit is enriched in As but in much lower concentrations than in the cobaltite ore at Blackbird, which typically contains more than 0.5 percent As. The low As content of the No-Name deposit relative to the Blackbird ore is a potentially significant economic factor because it allows more conventional smelting of sulfide concentrates. The No-Name deposit does not seem to be enriched in rare elements such as Nb, La, and Y, as is the Blackbird (Nash and Hahn, 1986), and no significant zones of Au enrichment have been identified at the No-Name deposit.

The composition of rocks containing fine-grained pyrite seems to differ in some fundamental ways from that of rocks containing coarse-grained pyrite. A test for differences between two groups of analyses grouped by general grain size of pyrite suggests that Al, Mg, and K concentrations are higher in the samples containing chiefly fine-grained pyrite, probably reflecting higher clay content, whereas total concentrations of S, Fe, Bi, Co, Cu, Ni, and Pb are higher in the samples containing chiefly coarse-grained pyrite. The suggestion that epigenetic pyritic samples contain higher concentrations of ore metals seems reasonable, but additional work is required to substantiate this generalization.

The chemistry of mineralized and barren samples from the No-Name deposit is consistent with petrographic features described previously, albeit on the basis of only 41 samples. The major-element composition, like the mineralogy, suggests mild alteration within the mineralized zones. The modest enrichment in chalcophile elements is logical for the highly sulfidic environment and consistent with the generally simple sulfide mineralogy. The details of residence of Bi, Pb, and Zn have not been established, but these trace constituents might reside in pyrite rather than as distinct minerals. The modest anomaly of barium in mineralized samples is not apparent in the mineralogy; no barite has been recognized, but the barium might reside in white micas or biotite.

Table 1. Analytical results for samples of drill core from the No-Name deposit, Lemhi County, Idaho

[Major elements in percent (%); minor elements in parts per million (ppm); s, determined by ICP; Fe_2O_3 computed from total iron reported as $FeTO_3$ minus iron determined as FeO; N, not detected at level shown; <, detected but below limit of determination shown; --, not determined; H, interference, nc: determined; LOI, loss on ignition (900 °C)]

Sample	SiO_2%	Al_2O_3%	Fe_2O_3%	FeO%	MgO%	CaO%	Na_2O%	K_2O%	TiO_2%	P_2O_5%	MnO %
IC3-0064	65.7	13.50	3.84	4.79	2.21	0.10	0.56	3.42	0.50	0.12	<0.02
IC3-0072	64.5	7.80	10.52	3.94	1.78	.10	.35	1.04	.30	.09	<.02
IC3-0083	60.4	12.30	5.26	6.70	2.36	.04	.63	3.76	.53	.08	.05
IC3-0102	57.2	15.30	2.68	10.10	3.11	.12	.34	4.82	.56	.11	.09
IC10-440	55.6	16.00	5.40	7.74	2.57	.09	.46	5.52	.63	.08	.06
IC10-806	65.1	12.20	8.53	7.09	1.63	.09	.26	4.91	.30	.10	.04
IC10-807	65.1	9.02	8.53	7.09	1.62	.09	<.15	3.91	.24	.07	.04
IC10-809	.H	.H	--	19.10	.H	.H	.H	.H	.H	.H	.H
IC10-819	.H	.H	--	12.10	.H	.H	.H	.H	.H	.H	.H
IC10-824	54.0	8.23	15.91	9.18	1.75	.14	.25	3.50	.29	.08	.05
IC10-829	71.2	10.20	2.67	6.26	1.70	.20	2.21	2.75	.30	.10	.04
IC12-265	64.3	10.90	--	.H	1.76	.17	<.15	4.32	.33	.10	.04
IC12-280	62.8	10.40	7.41	5.93	1.81	.16	.19	4.32	.39	.10	.05
IC12-285	55.6	9.41	12.53	5.73	1.74	.04	.16	2.96	.26	.10	.05
IC12-295	.H	.H	--	.H	.H	.H	.H	.H	.H	.H	.H
IC12-306	49.6	17.00	6.53	9.16	2.96	.15	1.18	4.86	.57	.15	.07
IC12-325	59.3	14.30	--	.H	2.70	.22	<.15	5.66	.61	.12	.08
IC12-328	64.4	14.60	2.61	6.14	2.17	.20	.60	5.41	.57	.16	.06
IC12-488	60.9	9.45	--	.H	1.44	.38	1.51	2.02	.17	.22	.04
IC16-236	56.9	14.30	4.09	8.20	2.77	1.44	2.14	3.81	1.17	.45	.14
IC16-244	53.3	13.40	8.85	7.52	2.51	.16	.45	4.86	.47	.11	.07
IC16-271	66.5	11.60	4.32	5.83	2.02	.09	.21	4.56	.35	.08	.06
IC16-281	61.7	9.43	8.46	5.98	1.71	.05	.19	3.46	.33	.06	.05
IC16-306	--	--	--	7.82	--	--	--	--	--	--	--
IC16-311	68.0	9.55	4.75	6.80	2.08	.13	.76	2.03	.34	.09	.07
IC16-336	64.8	11.70	--	.H	2.10	.17	1.26	2.96	.45	.09	.08
IC16-351	57.8	9.68	--	.H	2.81	.19	<.15	2.08	.33	.09	.13
IC16-542	59.4	10.50	--	.H	2.14	.16	.32	3.83	.37	.08	.11
IC18-700	66.3	13.20	1.61	7.82	2.58	.12	1.96	1.76	.45	.10	.05
IC18-762	63.1	12.50	3.71	6.29	2.21	.93	2.09	2.93	.89	.38	.07
IC18-767	59.5	13.70	8.20	6.30	2.29	1.14	1.80	3.92	1.06	.41	.08
IC18-768	59.5	13.70	4.55	6.80	2.29	1.14	1.80	3.41	1.06	.41	.08
IC18-770	.H	.H	--	.H	.H	.H	.H	.H	.H	.H	.H
IC18-781	60.3	13.80	--	.H	2.84	.29	1.08	3.08	.60	.11	.09
IC18-854	61.6	17.40	3.14	4.36	1.67	.14	1.30	5.86	.66	.10	.03
IC181064	65.0	12.30	6.03	4.65	1.39	.20	.96	4.39	.47	.08	.04
IC181068	71.9	10.60	4.03	4.04	1.26	.14	.49	3.96	.38	.08	.03
IC181074	66.6	12.50	4.70	4.86	1.43	.19	1.01	4.30	.46	.09	.04
IC181079	59.3	13.10	--	.H	2.15	.21	.93	4.47	.50	.10	.07
IC181080	69.0	13.00	4.46	4.02	1.33	.22	.98	4.58	.46	.10	.04
IC181081	68.5	13.00	3.99	4.14	1.31	.22	.98	4.58	.46	.09	.04

Table 1. Analytical results for samples of drill core from the No-Name deposit, Lemhi County, Idaho—Continued

Sample	Total C%	Total S%	LOI 900C	Al %-s	Fe %-s	Mg %-s	Ca %-s	Na %-s	K %-s	Ti %-s	P %-s
IC3-0064	<0.01	0.93	3.36	7.0	6.3	1.30	0.09	.36	2.80	.29	.050
IC3-0072	.02	5.64	6.78	4.2	11.0	1.10	.09	.22	.77	.17	.030
IC3-0083	<.01	3.36	4.84	6.6	9.0	1.40	.04	.44	3.10	.33	.030
IC3-0102	<.01	.47	3.11	7.5	8.9	1.70	.10	.20	3.50	.31	.040
IC10-440	<.01	2.66	4.06	8.8	10.0	1.50	.09	.30	4.50	.39	.030
IC10-806	.01	2.50	3.30	6.6	12.0	.97	.09	.17	4.00	.19	.040
IC10-807	.01	2.42	--	4.7	12.0	.95	.07	.04	2.90	.15	.030
IC10-809	.01	7.82	.H	1.2	56.0	.17	.02	.02	.60	.02	<.005
IC10-819	<.01	4.12	.H	3.4	28.0	.63	.07	.13	2.00	.12	.020
IC10-824	<.01	6.19	5.18	4.4	19.0	1.00	.10	.12	2.60	.18	.030
IC10-829	<.01	.93	1.40	5.5	6.9	1.00	.17	1.80	2.30	.19	.040
IC12-265	<.01	3.46	4.02	5.4	8.4	1.00	.11	.07	2.70	.20	.030
IC12-280	.02	4.46	4.69	5.4	9.7	1.00	.12	.07	3.20	.22	.040
IC12-285	<.01	9.83	8.14	5.3	14.0	1.10	.05	.07	2.50	.17	.040
IC12-295	<.01	19.30	.H	4.1	23.0	1.10	.11	.04	2.20	.26	.040
IC12-306	<.01	3.83	5.15	9.8	13.0	1.80	.14	.95	4.20	.37	.070
IC12-325	<.01	.77	2.62	7.2	9.0	1.60	.14	.07	3.50	.37	.040
IC12-328	<.01	.38	2.16	7.8	6.7	1.30	.17	.37	4.30	.34	.060
IC12-488	<.01	7.91	6.87	5.1	12.0	.89	.26	1.20	1.40	.12	.090
IC16-236	.17	1.31	3.27	7.4	9.1	1.60	1.00	1.50	3.00	.67	.200
IC16-244	<.01	6.11	5.99	7.9	13.0	1.60	.15	.30	4.30	.31	.050
IC16-271	<.01	1.65	3.04	6.0	7.4	1.20	.07	.10	3.40	.21	.030
IC16-281	<.01	6.05	5.98	5.2	11.0	1.00	.03	.06	2.70	.20	.020
IC16-306	.03	5.13	--	8.5	13.0	1.60	.13	.97	3.60	.32	.060
IC16-311	.05	2.24	3.64	5.0	8.5	1.20	.09	.53	1.50	.20	.040
IC16-336	.07	1.22	3.32	5.9	8.6	1.20	.11	.97	1.90	.28	.030
IC16-351	.20	4.16	6.43	4.7	14.0	1.60	.11	.05	1.30	.19	.030
IC16-542	.23	2.17	3.99	5.3	13.0	1.20	.10	.24	2.60	.23	.030
IC18-700	<.01	.15	2.61	7.1	7.3	1.50	.11	1.50	1.50	.27	.040
IC18-762	.15	1.88	3.06	6.8	7.6	1.30	.72	1.70	2.50	.55	.170
IC18-767	.20	4.95	6.11	7.3	11.0	1.30	.77	1.40	3.20	.62	.150
IC18-768	.20	2.04	3.84	6.9	8.1	1.30	.77	1.40	2.30	.62	.150
IC18-770	.17	24.00	.H	3.7	24.0	.64	.09	.22	1.40	.18	.030
IC18-781	.03	.87	3.55	7.0	9.3	1.70	.19	.85	2.20	.37	.040
IC18-854	<.01	.74	2.76	9.2	5.6	.96	.13	.97	4.70	.39	.040
IC181064	<.01	2.59	3.41	6.3	7.7	.81	.15	.64	3.30	.27	.040
IC181068	<.01	1.32	2.07	5.7	6.0	.73	.13	.35	3.20	.23	.030
IC181074	<.01	1.40	2.64	6.4	7.0	.82	.14	.70	3.30	.27	.040
IC181079	<.01	2.69	3.68	6.5	10.0	1.20	.14	.70	3.00	.30	.040
IC181080	<.01	1.74	2.76	7.2	7.1	.84	.14	.75	4.00	.28	.040
IC181081	<.01	.96	2.32	6.5	5.8	.74	.14	.75	1.40	.28	.040

Table 1. Analytical results for samples of drill core from the No-Name deposit, Lemhi County, Idaho—Continued

Sample	Ag ppm-s	As ppm-s	B ppm-s	Ba ppm-s	Be ppm-s	Bi ppm-s	Ce ppm-s	Co ppm-s	Cr ppm-s	Cu ppm-s
IC3-0064	<2	190	880	510	1	<10	17	540	52	2,700
IC3-0072	2	610	3,860	150	<1	50	68	2,400	200	3,600
IC3-0083	<2	90	500	200	1	<10	69	1,900	51	5,700
IC3-0102	<2	<10	90	370	<1	<10	270	290	45	2,300
IC10-440	<2	190	70	170	1	<10	130	1,200	74	140
IC10-806	<2	190	30	360	2	<10	41	1,200	120	47
IC10-807	<2	190	30	360	1	<10	27	1,200	120	47
IC10-809	<2	420	60	190	1	120	<4	3,300	100	11
IC10-819	<2	200	40	250	1	20	75	1,800	97	6
IC10-824	<2	300	60	190	1	20	79	2,700	100	35
IC10-829	<2	30	40	390	<1	<10	120	460	37	12
IC12-265	2	170	--	23	<1	10	180	1,500	37	6,200
IC12-280	<2	200	30	210	<1	<10	170	2,100	140	4,900
IC12-285	3	560	40	380	<1	<10	150	4,800	33	10,000
IC12-295	3	1,200	--	37	<1	70	110	10,000	48	5,100
IC12-306	<2	280	120	630	1	<10	460	2,100	69	2,600
IC12-325	<2	10	--	80	<1	<10	250	540	74	320
IC12-328	<2	<10	50	530	<1	<10	230	250	57	110
IC12-488	<2	530	--	13	<1	30	63	3,900	21	21
IC16-236	<2	50	40	650	1	<10	160	760	69	410
IC16-244	<2	330	40	910	<1	<10	150	3,600	55	3,000
IC16-271	<2	90	40	360	<1	<10	200	1,000	120	980
IC16-281	<2	390	40	210	<1	<10	77	3,300	150	6,800
IC16-306	<2	370	120	330	<1	20	240	2,600	140	1,800
IC16-311	<2	120	110	380	<1	10	170	1,200	130	980
IC16-336	<2	60	--	71	<1	<10	110	770	57	350
IC16-351	<2	240	--	20	<1	20	80	2,200	36	1,400
IC16-542	<2	140	--	30	<1	10	58	1,000	42	11
IC18-700	<2	<10	40	260	1	<10	37	70	40	1,100
IC18-762	<2	90	30	100	1	<10	66	760	27	410
IC18-767	<2	370	70	310	1	20	88	2,500	120	2,100
IC18-768	<2	120	40	38	1	10	88	900	37	370
IC18-770	5	1,700	--	10	<1	110	34	9,800	25	7,300
IC18-781	<2	<10	--	190	<1	<10	190	400	72	410
IC18-854	<2	30	50	190	1	<10	140	340	70	21
IC181064	<2	140	30	280	<1	<10	120	1,300	130	12
IC181068	<2	60	<20	52	<1	<10	110	650	39	2
IC181074	<2	70	20	490	<1	10	110	690	120	5
IC181079	<2	80	--	30	<1	10	120	1,200	54	27
IC181080	<2	90	20	74	<1	<10	130	880	54	6
IC181081	<2	60	20	68	<1	<10	110	490	54	3

Table 1. Analytical results for samples of drill core from the No-Name deposit, Lemhi County, Idaho—Continued

Sample	Eu ppm-s	Ga ppm-s	La ppm-s	Li ppm-s	Mn ppm-s	Mo ppm-s	Nb ppm-s	Nd ppm-s	Ni ppm-s	Pb ppm-s	Sc ppm-s
IC3-0064	<2	25	7	24	160	3	9	12	36	9	11
IC3-0072	<2	18	34	9	270	10	7	30	76	110	9
IC3-0083	<2	35	30	23	450	33	14	31	93	22	13
IC3-0102	3	42	120	29	690	2	13	110	34	7	11
IC10-440	<2	38	56	30	530	24	14	56	31	14	16
IC10-806	<2	27	18	20	370	21	8	18	33	8	9
IC10-807	<2	22	15	17	370	17	6	11	33	8	7
IC10-809	<2	18	2	5	230	<2	<4	<4	94	48	6
IC10-819	<2	18	39	13	250	11	5	35	51	13	6
IC10-824	<2	20	39	15	420	22	8	40	51	16	6
IC10-829	<2	18	57	15	390	3	6	53	22	8	6
IC12-265	3	25	91	20	390	3	--	81	38	10	6
IC12-280	3	25	84	19	450	7	6	78	40	11	6
IC12-285	<2	23	63	21	450	3	9	68	93	22	6
IC12-295	2	18	53	17	530	6	--	56	110	110	5
IC12-306	5	37	190	33	650	22	13	190	64	14	13
IC12-325	4	41	130	30	690	<2	--	120	44	8	12
IC12-328	3	39	110	28	520	2	11	92	28	5	13
IC12-488	<2	16	31	12	400	<2	--	29	25	40	4
IC16-236	3	29	85	24	1,100	14	29	73	41	28	9
IC16-244	<2	34	60	33	600	<2	12	60	75	37	9
IC16-271	2	25	96	27	500	5	7	94	34	11	8
IC16-281	<2	22	35	21	440	4	8	41	63	5	6
IC16-306	3	33	110	26	560	15	12	120	87	15	11
IC16-311	2	22	87	14	560	4	6	82	38	16	6
IC16-336	<2	27	58	18	680	6	--	51	34	5	9
IC16-351	<2	24	42	16	960	8	--	38	44	16	6
IC16-542	<2	29	29	18	860	12	--	28	37	10	7
IC18-700	<2	26	17	15	450	<2	9	15	28	6	10
IC18-762	<2	22	31	18	610	6	25	31	23	7	7
IC18-767	<2	33	46	22	640	11	10	44	49	11	8
IC18-768	<2	24	46	19	640	9	--	44	28	8	7
IC18-770	<2	18	17	11	490	12	--	16	290	91	3
IC18-781	2	38	100	19	710	<2	--	85	54	<4	12
IC18-854	<2	36	64	24	280	<2	15	51	7	6	18
IC181064	<2	26	61	17	350	10	7	55	33	9	10
IC181068	<2	22	50	16	310	9	8	45	17	6	7
IC181074	<2	26	56	16	380	9	6	54	24	8	8
IC181079	2	30	61	19	560	4	--	62	41	12	10
IC181080	<2	28	55	20	340	16	8	56	27	10	8
IC181081	<2	25	54	16	340	16	--	50	19	7	8

Table 1. Analytical results for samples of drill core from the No-Name deposit, Lemhi County, Idaho—Continued

Sample	Se ppm	Sr ppm-s	Th ppm-s	V ppm-s	Y ppm-s	Yb ppm-s	Zn ppm-s	Zr ppm-s	Au ppm
IC3-0064	--	29	12	53	9	1	53	254	0.05N
IC3-0072	31.0	88	8	50	12	2	50	146	.05
IC3-0083	--	28	12	48	14	2	69	269	.05N
IC3-0102	--	24	16	55	20	2	71	236	.05N
IC10-440	--	21	17	62	12	2	51	243	.05N
IC10-806	2.8	18	12	34	22	3	34	138	.05N
IC10-807	2.8	9	9	33	8	2	34	126	.05N
IC10-809	43.0	5	9	47	<2	<1	17	21	.05N
IC10-819	19.0	12	9	28	8	<1	27	147	.05N
IC10-824	17.0	16	8	40	9	1	32	145	<.05
IC10-829	--	69	9	23	12	1	26	116	.05N
IC12-265	19.0	18	9	21	15	2	63	--	.05N
IC12-280	19.0	20	7	21	10	1	80	168	.05N
IC12-285	--	15	12	21	15	2	66	136	.05N
IC12-295	70.0	14	12	24	6	1	60	--	.05N
IC12-306	--	44	14	60	25	3	91	209	.05N
IC12-325	9.3	19	14	55	20	3	51	--	.05N
IC12-328	--	28	15	60	17	2	37	209	.05N
IC12-488	24.0	31	8	18	12	2	31	--	.05N
IC16-236	4.6	190	12	46	27	3	120	277	.05N
IC16-244	--	31	13	37	24	3	76	184	.05N
IC16-271	7.2	17	8	27	16	2	54	175	.05N
IC16-281	27.0	12	7	21	10	1	67	159	.15
IC16-306	26.0	38	12	51	15	2	81	196	.05N
IC16-311	9.8	24	8	33	8	<1	140	150	.05N
IC16-336	9.9	35	12	43	11	1	49	--	.05N
IC16-351	17.0	15	8	47	14	2	68	--	.05N
IC16-542	15.0	16	8	47	13	2	34	--	.05N
IC18-700	--	30	12	42	11	2	55	203	.05N
IC18-762	--	73	10	35	11	1	51	253	.05N
IC18-767	18.0	76	14	41	12	2	57	272	.05N
IC18-768	14.0	76	11	41	12	1	57	245	.05N
IC18-770	87.0	15	9	18	4	<1	52	--	.05N
IC18-781	7.7	32	12	63	14	2	58	--	.05N
IC18-854	--	43	15	74	12	2	30	231	.05N
IC181064	7.6	35	11	39	24	3	23	203	.05N
IC181068	--	29	7	31	23	2	18	161	.05N
IC181074	4.7	31	12	39	16	2	23	196	.05N
IC181079	14.0	28	10	49	20	3	35	--	.05N
IC181080	6.3	34	9	41	19	3	22	215	.05N
IC181081	6.3	34	9	41	16	2	19	239	.05N

Table 2. Summary of analytical results for ore and enclosing wallrocks, No-Name deposit, Lemhi County, Idaho

[Oxides in percent, rest parts per million; n, number of valid determinations; n for many major elements determined by X-ray fluorescence is reduced by interference caused by high iron concentrations; L, less than value shown; $FeTO_3$, total iron expressed as ferric iron, determined by ICP; **, not computed, too few valid determinations]

Element	Co-pyrite zones				Barren hangingwall and footwall zones			
	n	min.	max.	geom. mean	n	min.	max.	geom. mean
SiO_2	21	49.6	68.0	60.8	15	59.3	71.9	63.4
Al_2O_3	21	7.8	17.0	11.6	15	9.5	17.4	12.5
$FeTO_3$	26	9.0	80	17.3	15	8.0	18.6	11.6
MgO	21	1.4	3.1	2.1	15	1.3	2.6	1.9
CaO	21	.04	1.4	.15	15	.04	1.1	.23
Na_2O	21	.16L	2.1	.54	13	.15L	2.2	1.0
K_2O	21	1.04	5.5	3.4	15	2.0	5.9	3.9
TiO_2	21	.24	1.2	.43	15	.17	1.1	.5
P_2O_5	21	.06	.45	.11	15	.08	.41	.13
S total	26	.15	24.0	3.1	15	.38	7.9	1.6
C total	12	.01L	.20	.02	4	.03L	.23	.02L
Ag	4	2L	5	**	1	2	2	**
As	24	50	1,700	242	13	10L	530	76
Au	3	.05L	.15	**	0	.05L	.05L	**
B	22	20	3,860	68	8	20L	500	41
Ba	26	10	910	221	15	13	530	79
Bi	11	10L	120	13	5	10L	30	10L
Co	26	70	10,000	1,586	15	250	3,900	774
Cr	26	25	200	80	15	21	74	46
Cu	26	5	10,000	532	15	2	6,200	70
Mn	26	160	1,100	463	15	280	860	473
Mo	23	2L	24	9	11	21	33	7
Pb	26	5	110	16	14	5L	40	9
Se	19	2	87	14	9	6.3	24	12
V	26	18	62	37	15	18	74	40
Zn	26	17	140	52	15	18	69	37

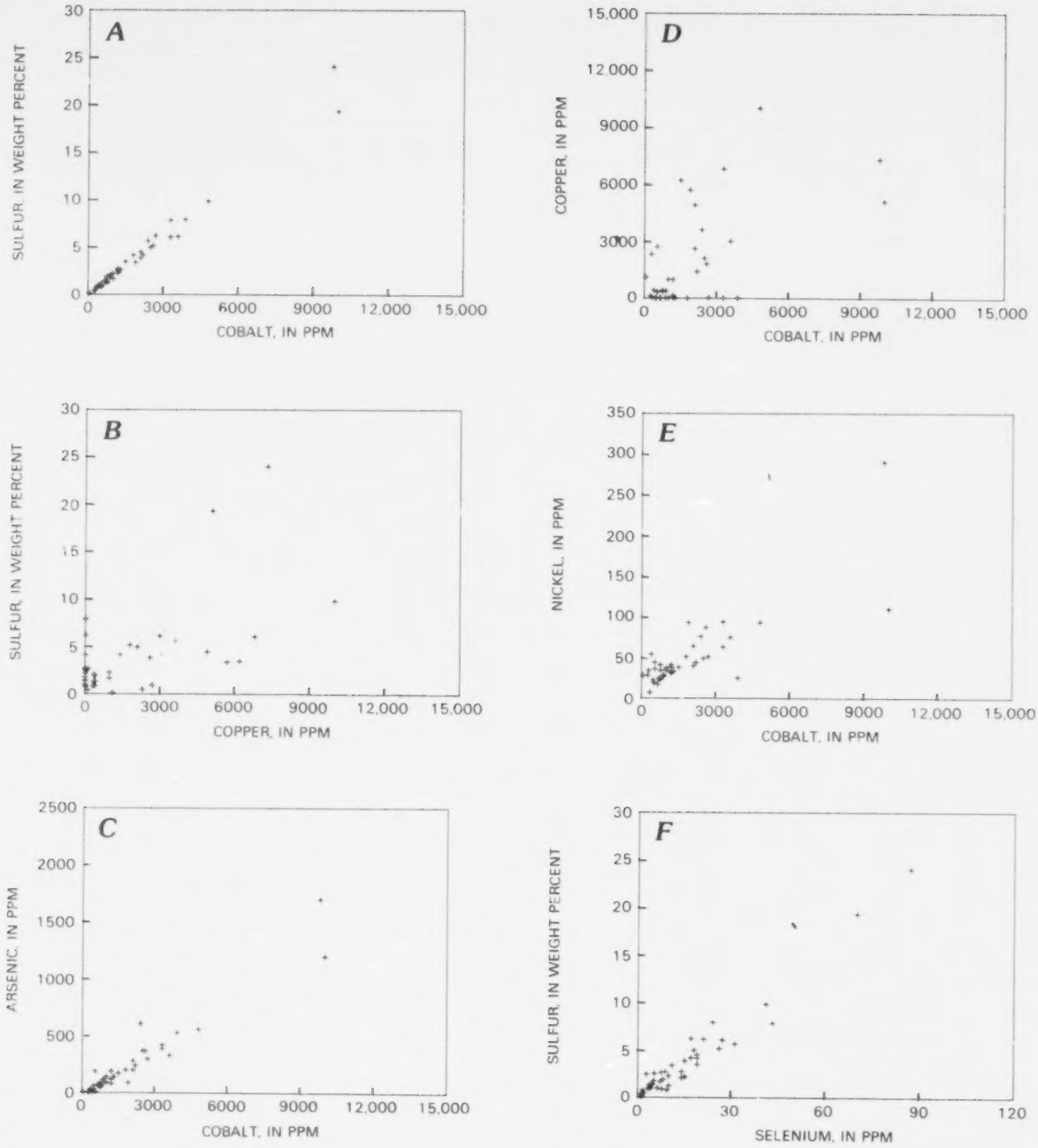

Figure 7. Scatterplots of geochemical data for the No-Name deposit. *A*, Plot of cobalt against sulfur. The linear relation supports mineralogical evidence that cobalt substitutes for iron in pyrite rather than occurring as a distinct cobalt mineral. *B*, Plot of copper against sulfur. *C*, Plot of cobalt against arsenic. Although there is a linear relation of cobalt and arsenic, this relation actually reflects the control on both cobalt and arsenic by their incorporation in pyrite rather than their presence as a distinct cobalt-arsenic mineral. *D*, Plot of cobalt against copper showing lack of linear relation at higher concentrations of cobalt and copper. *E*, Plot of cobalt against nickel. The occurrence of nickel, like cobalt, is controlled by pyrite. *F*, Plot of selenium against sulfur. The linear relation implies that selenium occurs in pyrite rather than as a distinct selenium mineral.

DISCUSSION AND INTERPRETATION

Environment of Formation

The cobalt deposits of the Iron Creek area formed during and shortly after sedimentation in an unstable part of the Yellowjacket rift basin. Although there is some valid evidence for shallow-water sedimentation not far from the deposits (Modreski, 1985), strata that are mineralized are darker and were deposited below wave base. Some paleocurrent measurements indicate deposition was from the east, and the cobaltiferous zones at Iron Creek seem to have been in the central part of the northwest-trending rift basin (Hughes, 1983). Slump folds and synsedimentary deformation between undisturbed strata were produced by gravitational instability on the submarine fan. Mafic dikes and probable mafic volcaniclastic rocks suggest that volcanism accompanied sedimentation, but volcanic rocks are more abundant to the north in the vicinity of the Blackbird mine (Hahn and Hughes, 1984; Nash and Hahn, 1986).

Synsedimentary Structural Controls

Cobaltiferous pyrite zones favor disruption structures that formed prior to consolidation. Substantial amounts of magnetite and fine pyrite are stratiform or appear to have been part of the sediment prior to disruption; these early stages of mineralization, possibly syngenetic, contain only small amounts of cobalt. Thus, the synsedimentary structures provide key evidence for the timing and character of processes that introduced and deposited cobalt.

Strata containing Co-pyrite also contain resedimented clastic grains and rounded clasts of partly consolidated sediment. As described earlier, most of the structures are concordant: they are confined between undisturbed beds, and the planar or linear features of their fabrics are aligned parallel to the dip of beds. In contrast, other mineralized structures are discordant: they cut across beds and indicate injection of unconsolidated material by upward-moving pore fluids that perhaps had sufficient velocity to meet the definition of fluidization (Lowe, 1975). Most of the transported material seems to have been only slightly suspended or liquefied and in that state was gravitationally unstable. Magnetite appears to have been especially unstable because very little of it is bedded, yet almost certainly it was originally a chemical sediment in beds a few millimeters to more than 1 m thick. Although details required to quantify specific behavior as plastic, liquefied, thixotropic, or fluidized are difficult to obtain and certainly are debatable, the qualitative conclusion that the deformation and associated mineralization occurred prior to consolidation seems valid.

Cobalt enrichment was not strictly syngenetic but occurred early in the history of the host rocks. If clastic dikes form at depths of about 30–60 m (Dzulynski and Randomski, 1956; Hiscott, 1979), we can infer comparable conditions of very shallow burial for these structures at Iron Creek. Pore fluids clearly moved through these structures—indeed, were instrumental in producing them. The physical principles of liquefaction and fluidization (Lowe, 1975) imply geologically brief periods of elevated pore pressure and fluid injection. However, there is no way to count the number of fluid pulses or relate the specific time of formation of zones 10 or 100 m apart. It is likely that the fluid pulses were episodic. Earthquakes are typically cited as causes (Lowe, 1975), but I would add slumping and volcanic eruptions as known Yellowjacket events that could have triggered fluid injection. In summary, this was a dynamic system of reactive unconsolidated sediment containing abundant pore fluid that was gravitationally unstable and was heated by a small volcanic system.

There are few examples in the literature of similar synsedimentary controls on ore deposits. Descriptions of "quickstone" containing "pelletoid conglomerate," folded and "flowsheared" fabric, and gravity slides (McNeil, 1966) at the Orlando mine, Tennant Creek, Australia, seem similar to features of the No-Name deposit. (The Tennant Creek deposits also are rich in magnetite and provide a useful geochemical as well as structural analogy for the Iron Creek deposit.) Soft-sediment deformation of quartzite and argillite in the Belt Supergroup (Middle Proterozoic) at the Atlas mine, Coeur D'Alene mining district, Idaho, was reported by Chevillon (1977); the deformation was associated with synsedimentary movement of a major fault strand related to the regionally important Osborne fault. The faulting, soft-sediment deformation, and focus of fluids are part of the early stages of ore deposition. Sedimentary and early diagenetic structures are distinguished (Jonasson and Goodfellow, 1986) from tectonic ones in the Howards Pass zinc-lead deposit, where disharmonic folds having no axial-planar cleavage are common and considered diagnostic of synsedimentary deformation; such structures were suspected in the No-Name deposit but small folds of any type are very rare. Well-exposed features such as ore clasts, ore breccia, folded beds, and gravity-slide blocks in Kuroko massive-sulfide deposits indicate deformation penecontemporaneous with ore formation on the sea floor (Hashiguchi, 1983). This deformation is related to intrusion of rhyolite, doming, and phreatic explosions. On the other hand, McClay (1983) points out that many fold structures in sediment-hosted ore

deposits that some think are synsedimentary are actually of tectonic origi . as determined by microstructural criteria such as ductile deformation of sulfides. McClay (1983) does describe some synsedimentary structures that displace ore minerals and notes that one of the most reliable tests for this early age is crosscutting dewatering structures.

Geochemistry

The most notable chemical feature of the Iron Creek deposits is the high concentration of iron. Iron was deposited in several stages as chemical sediment interbedded with siliciclastic and volcaniclastic sediments. Regionally, this is but one cluster of iron-rich sedimentary deposits that trend northwesterly from the iron deposits at McKim Creek (Soregaroli, 1961), about 18 km southeast of the No-Name deposit, through the Idaho cobalt belt (Hughes, 1983), with many occurrences of rocks rich in iron oxides or silicates, and possibly as far north as the bedded magnetite deposits at Woods Creek, Ravalli County, Mont. (about 90 km north of the study area). Introduction of iron into the Yellowjacket basin, probably from thermal vents, seems to be a regional manifestation of the rift system described by Hughes (1983).

The ferruginous sediments accumulated during periods of mostly low energy sedimentation as beds a few millimeters thick to aggregates more than 3 m thick. The aggregated beds of magnetite outline local subbasins having strike lengths of more than 1.5 km in the Jackass and No-Name zones; the width of these zones is not known in detail but must have been hundreds of meters. The surges of iron-rich hydrothermal fluids first caused the deposition of iron oxides and very little or no sulfide minerals. Concentrations of cobalt, copper, and other ore metals possibly were very low in the oxide stage; clearly, very small amounts of ore metals were deposited. The lack of sulfide minerals probably relates to lack of sulfur rather than to oxidation because there are only small amounts of hematite to suggest oxidizing conditions. Later in each period of ferruginous exhalation, sulfide became available. This caused the formation of iron-sulfide muds, now fine-grained stratiform pyrite. Some cobalt was co-deposited with the sulfide mud. The ferruginous muds were unstable on the seafloor and were the focus of sliding, liquefaction, and occasional fluid injection into overlying beds. Diagenetic reactions caused recrystallization to fine well-formed grains of magnetite and pyrite. Pore fluids expelled from the compacting pile caused the liquefaction and carried iron, cobalt, and copper, but low concentrations of other metals. These processes of iron exhalation and sedimentation, buildup of sulfide, liquefaction and sliding, and deposition of Co-pyrite and chalcopyrite were repeated many times during the accumulation of 400 m of siliciclastic sediments in the No-Name zone.

The Co-pyrite deposits are enriched in a limited suite of chalcophile elements. The most significant is copper, accompanied by very minor amounts of silver, lead, and zinc. Bismuth is notably concentrated, as is arsenic, but arsenic is not nearly as abundant as in the Blackbird deposits. These elements seem to have been introduced by diagenetic pore fluids, not by a fluid erupted on the seafloor. As explained above, episodic movement of pore fluid through the unconsolidated sediments seems likely. It is possible that the quiescent periods allowed leaching and equilibration with the sediment and also may have allowed a buildup of sulfide ion, perhaps by bacterial action. During periods of fluid flow through the synsedimentary structures, the chalcophile ions reacted with sulfide ions to form sulfide minerals, some of which were rich in cobalt. Details of the reactions are not known. The fluids appear to have been in equilibrium with the host rocks because no unusual alteration is found in association with the sulfides; thus, a mechanism such as change in pH does not seem to have caused sulfide deposition. Stable isotopic studies might provide constraints on the sulfur cycle and deposition mechanisms.

Similar Ore Deposits

The synsedimentary controls, mineralogy, and geochemistry of the Iron Creek deposits seem to be unusual among ore deposits, but similar features are known in some. Sediment-hosted deposits are major ore producers in many parts of the world (Stanton, 1972), but most tend to be rich in lead and zinc. Some that are rich in copper also contain significant amounts of cobalt. Most notable are the many important deposits of the Zambian Copperbelt, which is the major source of cobalt for the Western World (Annels and Simmonds, 1984). Cobalt is not uniformly distributed at regional or deposit scale but is mostly confined to a belt about 100 km long by 10 km wide, probably coincident with a rift zone (Annels and Simmonds, 1984). Cobalt in the Zambian deposits is always with copper—no cobalt-only deposits are known—and generally is most abundant in the central part of the copper-cobalt deposits. Much of the cobalt occurs in pyrite, some individual grains or growth zones containing more than 20 percent Co. Other hosts for cobalt include cobaltite and a variety of cobalt-copper-nickel sulfide minerals. A source of cobalt and copper in mafic igneous rocks in the rift zone is advocated (Annels and Simmonds, 1984). A major difference between the African and Idaho cobalt-copper deposits is the shallow-water sedimentary features in the

Zambian Copperbelt sediments and the abundant diagenetic anhydrite that reacted to form sulfide minerals (Annels, 1974; Annels and Simmonds, 1984).

The world-class base-metal deposits at Mount Isa and Broken Hill, Australia, thought by some to be synsedimentary in origin prior to severe deformation and metamorphism (Stanton, 1972), have some intriguing similarities to the deposits of the Idaho cobalt belt and contain local enrichments of cobalt. In the Mount Isa lead-zinc-copper deposits (Croxford, 1974) cobalt is locally concentrated to about 300 ppm and in a few rare places exceeds 1 percent. The cobalt is associated with zones rich in copper and is present as cobaltite and other cobalt-arsenic-sulfur minerals. The copper and cobalt are interpreted to have moved during metamorphism (Croxford, 1974), so their original residence is not known for comparison with the No-Name deposit. No significant cobalt has been found in the Mount Isa pyrite.

The deposits of Tennant Creek, Australia (Large, 1975, 1976), important producers of gold, may provide a useful geologic or geochemical analog. The Tennant Creek deposits are notably rich in magnetite (that forms as much as 80 percent of central ore zones), bismuth, and selenium, as well as gold. Although importance of syngenetic deposition of magnetite is a subject of debate (Dunn, 1976), the Tennant Creek deposits provide a useful exploration model for possible gold in the Iron Creek deposits. Assays to date have not found gold of significant concentration (>1 g/t) or volume. Gold at Tennant Creek (Large, 1975) is found in the central part of the zoned mineralized area in magnetite-chlorite rock, a bismuth zone being nearby; copper and sulfur are most abundant outside the gold zone. The gold-magnetite-chlorite orebodies occur above chlorite-rich alteration pipes that probably were feeders; comparable alteration or likely feeder structures have not been identified in the Iron Creek deposits. Ore-forming conditions at Tennant Creek were more oxidizing than in typical sulfide deposits such as volcanogenic massive-sulfide deposits that are similar in many ways to Tennant Creek (Large, 1976). Oxidizing conditions may be a requirement for that magnitude of gold transport and deposition. Although not emphasized by Large (1975, 1976), at least some deposits in the Tennant Creek district display evidence for synsedimentary soft-sediment deformation (McNeil, 1966) that seems similar to features in the Iron Creek area.

Metamorphism

Regional greenschist metamorphism seems to have had little or no effect on the Iron Creek mineralization. The silicate mineral assemblage is essentially the same within deposits as it is outside, and the fabric of the ore minerals seems consistent with deposition or recrystallization in a shallow geothermal system. The late paragenetic position of chalcopyrite and the presence of a copper-rich zone above the Co-pyrite zone in the No-Name deposit might reflect remobilization of copper during metamorphism, which commonly occurs, but also could be explained by later deposition of copper in the submarine system. The prominent cleavage in the area does not seem to influence ore minerals, and its age and origin is not known.

Resources and Exploration

The No-Name deposit has been a subeconomic resource in the recent cobalt market. If the price of cobalt were to increase substantially, or if cobalt cannot be supplied by foreign sources, the deposit could supply cobaltiferous-pyrite concentrate that could be smelted in existing United States facilities. The partially drilled resource is about 1 million tons and has a grade in excess of 0.5 percent Co (Webster and Stump, 1980), or about 6 million kg cobalt metal. Depending upon economic factors, lower grade or thinner parts of the deposit, as well as downdip and on-strike extensions, might add substantially to this resource.

The more general question is what additional Co-pyrite resources might exist and be discoverable. Certainly the very poor outcrop in the Idaho cobalt belt has prevented recognition of deposits. Although gossan is visible in the Jackass and No-Name zones, the zones attracted attention after being cut, quite by chance, by logging roads. Despite the poor exposure, several lenses of magnetite iron-formation are known in the cobalt belt, but only one has abundant Co-pyrite. The magnetite is a useful exploration feature because it is easily detected by magnetic surveys. The cobalt deposits also create strong geochemical anomalies in soil and in water (Erdman and Modreski, 1984) and should be detectable. Economic incentives are required to do the detailed exploration needed to locate and drill new prospects.

There are several reasons to postulate the existence of many additional Co-pyrite zones similar to the No-Name. Many stratiform and discordant iron deposits are known along the more than 60-km strike length of the cobalt belt; these are indicators of hydrothermal vents along the rift zone. The starved-basin stage of the Yellowjacket basin (Hughes, 1983) is conceptually conducive to the accumulation of widespread pyritic sediment that would be a favorable component in making Co-pyrite deposits. Finally, the soft-sediment deformation and dewatering phenomenon that seem to be important in creating rich Co-pyrite zones are widespread in the lower and middle units of the Yellowjacket Formation and extend well beyond areas where they are known to be associated with cobalt deposits.

Exploration for gold in the Iron Creek area should be directed at identifying structures and alteration indicative of focused hydrothermal activity. According to the Tennant Creek example, gold might be expected to be richest in zones of magnetite, but in other types of iron-rich sedimentary sequences gold deposition favors the transition from oxide to sulfide facies (see, for example, Fripp, 1976).

Ore Genesis

The low-temperature transport of cobalt is not as well understood as that of most base metals in sedimentary environments (see, for example Lydon, 1983). Thermochemical models (Haynes and Bloom, 1987) predict that base-metal ratios can be explained by composition of the source rock, oxygen fugacity of the transporting brine, and sulfur fugacity at the site of deposition. The very high cobalt : copper of the No-Name deposit, and low concentration of silver, lead, and zinc might be explained by a mafic source rock, moderate oxygen fugacity during leaching and transport, and high sulfur fugacity during deposition. There is experimental evidence that stable cobalt-chloride complexes form at temperatures of about 100–200 °C and are stronger than those of nickel-chloride (Susak and Crerar, 1985). This provides a mechanism for the separation of cobalt from nickel and explains the unusually high cobalt : nickel in the Co-pyrite as well as in the Blackbird deposits. The cobalt-chloride complexes weaken rapidly with decrease in temperature; thus, cooling should be a viable process for deposition as long as the requirements for reduced sulfur are met.

Cobalt deposition might possibly have been triggered by mixing of a heated subsurface cobalt-bearing brine with cooler seawater. If cobalt was complexed by chloride in a saline brine, which could also have contained a limited amount of sulfide ion, mixing with seawater on the sea floor or in the disruption structures would have cooled the brine and also decreased the concentration of chloride—both processes would have destabilized cobalt-chloride complexes and permitted reaction with any available sulfide ions. Such a mechanism also would have promoted transport and deposition of iron and copper.

Details of the hydrothermal plumbing system are lacking. Drill data suggest that much of the flow was subhorizontal in disruption zones confined between undeformed strata. No feeder faults or associated discordant alteration zones are known, although this might be explained by poor exposure and the small cross section encountered by drill holes oriented perpendicular to bedding. Also, it is possible that the deposit slid basinward from the vents. Given the present steep dip of beds and the likelihood of submarine slides (or aggregate of small slips), the concept of drilling "closer to the vent" in search of thicker Co-pyrite zones or higher gold concentrations is not easily accomplished.

REFERENCES CITED

Annels, A.E., 1974, Some aspects of the stratiform ore deposits of the Zambian Copperbelt and their genetic significance, *in* P. Bartholome, ed., Gisements stratiformes et provinces cupriferes: Liege, Société Géologique de Belgique, p. 235–254.

Annels, A.E., and Simmonds, J.R., 1984, Cobalt in the Zambian Copperbelt: Precambrian Research, v. 25, p. 75–98.

Chevillon, C.V., 1977, Tectonically induced, Proterozoic soft sediment deformation at the Atlas property, Coeur D'Alene mining district, Idaho: Geological Society of America Abstracts with Programs, v. 9, no. 6., p. 716.

——— 1979, Iron Creek project progress report (1977–1978): Unpublished report, Noranda Exploration, Inc., 56 p. (geologic map, scale 1:4,800).

Cohenour, R.E., Fox, R.C., and Robison, W.D., 1973, Geology and geophysics of the Iron Creek copper-cobalt deposit, Lemhi County, Idaho: American Institute of Mining, Metallurgical, and Petroleum Engineers, Pacific Northwest Metals and Minerals Conference, 1973, Coeur D'Alene, Idaho, 15 p.

Croxford, N.J.W., 1974, Cobalt mineralization at Mount Isa, Queensland, Australia, with references to Mount Cobalt: Mineralium Deposita, v. 9, p, 105–115.

Davis, J.C., 1986, Statistics and data analysis in geology: New York, John Wiley and Sons, 646 p.

Dunn, P.G., 1976, Zonation of hydrothermal minerals at the Juno mine, Tennant Creek goldfield, central Australia—A discussion: Economic Geology, v. 71, p. 1614–1615.

Dzulynski, S., and Randomski, A., 1956, Clastic dikes in Carpathian flysch: Rocznik Polskiego Towarzystwa Geologicznego, v. 26, p. 225–273.

Elliott, R.E., 1965, A classification of subaqueous sedimentary structures based on rheological and kinematical parameters: Sedimentology, v. 5, p. 193–209.

Erdman, J.A., and Modreski, P.J., 1984, Copper and cobalt in aquatic mosses and stream sediments from the Idaho cobalt belt: Journal of Geochemical Exploration, v. 20, p. 75–84.

Fripp, R.E.P., 1976, Stratabound gold deposits in Archean banded iron formation, Rhodesia: Economic Geology, v. 71, p. 58–75.

Hahn, G.A., and Hughes, G.J., Jr., 1984, Sedimentation, tectonism, and associated magmatism of the Yellowjacket Formation in the Idaho cobalt belt, Lemhi County, Idaho, *in* Hobbs, S.W., ed., The Belt, abstracts with summaries, Belt symposium II, 1983: Montana Bureau of Mines and Geology Special Publication 90, p. 65–67.

Hashiguchi, Hironori, 1983, Penecontemporaneous deformation of Kuroko ores at the Kosaka mine, Akita, Japan, in Ohmoto, Hiroshi, and Skinner, B.J., eds., The Kuroko and related volcanogenic massive sulfide deposits: Economic Geology, Monograph 5, p. 167–183.

Haynes, D.W., and Bloom, M.S., 1987, Stratiform copper deposits hosted by low energy sediments—IV. Aspects of sulfide precipitation: Economic Geology, v. 82, p. 875–893.

Hiscott, R.N., 1979, Clastic sills and dikes associated with deep-water sandstones, Tourelle Formation, Ordovician, Quebec: Journal of Sedimentary Petrology, v. 49, p. 1–9.

Hubbert, A.E., and Chao, T.T., 1985, Determination of gold, indium, tellurium, and thallium in the same sample digestion of geological materials by atomic absorption spectroscopy and two-step solvent extraction: Talanta, v. 32, p. 568–570.

Hughes, G.J., Jr., 1983, Basinal setting of the Idaho cobalt belt, Blackbird mining district, Lemhi County, Idaho, *in* The genesis of Rocky Mountain ore deposits—Changes with time and tectonics: Denver Region Exploration Geologists Society, p. 21–27.

Jackson, L.L., Brown, F.W., and Neil, S.T., 1987, Major and minor elements requiring individual determinations, classical whole rock analysis and rapid rock analysis, *in* Baedecker, P.A., ed., Methods for geochemical analysis: U.S. Geological Survey Bulletin 1770, p. G1–G23.

Jonasson, I.R., and Goodfellow, W.D., 1986, Sedimentary and diagenetic textures, and deformation structures within the sulfide zone of the Howards Pass (XY) Zn-Pb deposit, Yukon and Northwest Territories, *in* Morin, J.A., ed., Mineral deposits of northern Cordillera: Canadian Institution of Mining and Metallurgy Special Volume 37, p. 51–70.

Large, R.R., 1975, Zonation of hydrothermal minerals at the Juno mine, Tennant Creek goldfield, central Australia: Economic Geology, v. 70, p. 1387–1413.

_____ 1976, Zonation of hydrothermal minerals at the Juno mine, Tennant Creek goldfield, central Australia—A reply: Economic Geology, v. 71, p. 1615–1617.

Lichte, F.E., Golightly, D.W., and Lamothe, P.J., 1987, Inductively coupled plasma–atomic emission spectrometry, *in* Baedecker, P.A., ed., Methods for geochemical analysis, U.S. Geological Survey Bulletin 1770, p. B1–B10.

Lowe, D.R., 1975, Water escape structures in course-grained sediments: Sedimentology, v. 22, p. 157–204.

Lydon, J.W., 1983, Chemical parameters controlling the origin and deposition of sediment-hosted stratiform lead-zinc deposits, *in* Sangster, D.F., ed., Short course in sediment-hosted stratiform lead-zinc deposits: Mineralogical Association of Canada, v. 8, p. 175–250.

McClay, K.R., 1983, Deformation of lead-zinc deposits, *in* Sangster, D.F., ed., Short course in sediment-hosted stratiform lead-zinc deposits: Mineralogical Association of Canada, v. 8, p. 283–309.

McNeil, R.D., 1966, Geology of the Orlando mine, Tennant Creek, Australia: Economic Geology, v. 61, p. 221–242.

Middleton, G.V., and Hampton, M.A., 1973, Sediment gravity flows—Mechanics of flow and deposition, *in* Turbidites and deep water sedimentation: Society of Economic Paleontologists and Mineralogists, Pacific Section Short Course, p. 1–38.

Modreski, P.J., 1985, Stratabound cobalt-copper deposits in the Middle Proterozoic Yellowjacket Formation in and near the Challis quadrangle, *in* McIntyre, D.H., ed., Symposium on the geology and mineral deposits of the Challis 1°×2° quadrangle, Idaho: U.S. Geological Survey Bulletin 1658, p. 203–222.

Mottl, M.J., 1983, Metabasalts, axial hot springs, and the structure of hydrothermal systems at mid-ocean ridges: Geological Society of America Bulletin, v. 94, p. 161–180.

Nash, J.T., and Hahn, G.A., 1986, Volcanogenic character of sediment-hosted Co-Cu deposits in the Blackbird mining district, Lemhi County, Idaho—An interim report: U.S. Geological Survey Open-File Report 86–430, 29 p.

Ramdohr, Paul, 1980, The ore minerals and their intergrowths, 2nd edition: New York, Pergamon Press, 1205 p.

Soregaroli, A.E., 1961, Geology of the McKim Creek area, Lemhi County, Idaho: Moscow, University of Idaho, M.S. thesis, 53 p.

Stanton, R.L., 1972, Ore petrology: New York, McGraw-Hill, 713 p.

Susak, N.J., and Crerar, D.A., 1985, Spectra and coordination changes of transition metals in hydrothermal solutions—Implications for ore genesis: Geochimica et Cosmochimica Acta, v. 49, p. 555–564.

Swarbrick, E.E., 1968, Physical diagenesis; intrusive sediment and connate water: Sedimentary Geology, v. 2, p. 161–175.

Taggart, J.E., Jr., Lindsay, J.R., Scott, B.A., Vivit, D.V., Bartel, A.J., and Stewart, K.C., 1987, Analysis of geologic materials by wave-length dispersive X-ray fluorescence spectrometry, *in* Baedecker, P.A. ed., Methods for geochemical analysis: U.S. Geological Survey Bulletin 1770, p. E1–E19.

Webster, T.A., and Stump, T.K., 1980, Iron Creek prospect, Lemhi County, Idaho: Unpublished report, Noranda Exploration, Inc., 46 p.

Wilson, S.A., Kane, J.S., Crock, J.G., and Hatfield, D.B., 1987, Chemical methods of separation for optical emission, atomic absorption, and colorimetry, *in* Baedecker, P.A., ed., Methods for geochemical analysis: U.S. Geological Survey Bulletin 1770, p. D1–D9.

APPENDIXES 1 AND 2

APPENDIX 1. DESCRIPTION OF ANALYZED SAMPLES

[P, petrographic analysis; C, chemical analysis]

IC3–64	[P,C] Weakly laminated siltite and fine quartzite; muscovite more abundant than biotite; contains knots of carbonate minerals that cut bedding.
IC3–72	[C] Weakly laminated siltite and argillite; cobalt zone.
IC3–83	[P,C] Partly bedded siltite and argillite containing sandy dikelets; some beds of fine pyrite (pyrite mud?).
IC3–102	[C] Laminated siltite.
IC3–113	[P] Weakly to nonbedded argillite and minor siltite containing sand dikelets; some beds of fine pyrite mud.
IC10–440	[P,C] Laminated siltite above cobalt zone; cut by gash fractures filled by quartz.
IC10–448	[P] Disruption 1 ft thick filled by coarse pyrite, quartz, and green mica (chlorite after biotite).
IC10–460	[P] Disrupted nonbedded zone hard from silicification; quartz and muscovite are coarse (300μm) and recrystallized.
IC10–496	[P] Greenstone (chlorite-epidote-plagioclase rock) containing weakly aligned crystals; altered mafic dike or pyroclastic.
IC10–806	[C] Laminated argillite above magnetite zone.
IC10–807	[C] Split of sample IC10–806.
IC10–809	[P,C] Disruption zone rich in magnetite; layers of fine and coarse magnetite, pyrite, or magnetite and pyrite.
IC10–814	[P] Partly layered zone, mostly disruption-filling magnetite and pyrite, with minor siliciclastic component; quartz cements ore minerals.
IC10–819	[C] Base of disruption zone, just above laminated siltite; magnetite and pyrite fill disruption.
IC10–821	[P] Footwall to major disruption zone; sample is lumpy disruption with sausage-shaped infilling of magnetite that probably was folded during compaction; laminated siltite contains much more pyrite than magnetite, but infill contains much more magnetite than pyrite.
IC10–824	[C] Disruption zone rich in magnetite and containing 10 percent pyrite; bedding appears stirred or smeared with 2-cm lumps of sediment.
IC10–829	[P,C] Lumpy disrupted argillite with dikelets of sand-sized quartz and magnetite, cemented by quartz and biotite (retrograded to chlorite).
IC12–234	[P] Disruption structure filled by coarse pyrite; wallrock siltite and argillite are recrystallized to coarse grains of quartz and mica; fabric is weakly gneissic (from slip?). This is at top of an 88-ft-thick sequence of mostly disrupted sediment.
IC12–265	[P,C] Weakly laminated siltite and lumps of argillite; coarse veinlike quartz and pyrite fill openings.
IC12–270	[P] Disruption zone filled by coarse pyrite and much less chalcopyrite, quartz, and chlorite (replaced biotite). No magnetite. Chalcopyrite engulfs pyrite.
IC12–280	[C] Disrupted zone containing coarse pyrite and chalcopyrite.
IC12–285	[C] Disrupted zone, abundant coarse pyrite and chalcopyrite.
IC12–295	[C] Pyrite-rich (50 percent) filling of 1-ft-wide disruption.
IC12–305	[P,C] Layered fine-grained pyrite in argillite; pyrite mud(?).
IC12–325	[P,C] Footwall to disruption zone, laminated siltite containing little pyrite.
IC12–328	[P,C] Footwall of ore zone, laminated argillite, scattered sand dikelets.
IC12–488	[P,C] Laminated fine-grained pyrite in argillite; pyrite mud(?).
IC12–623	[P] Massive textured rock from 619- to 657-ft depth; equal amounts of plagioclase, chlorite, and epidote, and abundant fine magnetite; phenocryst texture survives; mafic dike.
IC16–236	[C] Laminated siltite and fine quartzite, low sulfide content, example of hangingwall.
IC16–244	[C] Laminated siltite containing little sulfide, background reference.

IC16–271 [C] Mostly laminated siltite and a few centimeter-size disruptions containing sulfides.

IC16–281 [C] Moderately disrupted siltite, some bedding is normal; disruptions filled with pyrite.

IC16–290 [P] Highly disrupted zone in which lumps of argillite are cemented by coarse (200 μm) sand and chemical quartz; contains much more pyrite than chalcopyrite, chalcopyrite surrounds euhedral pyrite; no magnetite.

IC16–296 [P] Disruption zone filled by coarse pyrite; crystals of pyrite are broken and corroded, cemented by quartz and biotite (altered to chlorite). Texture suggests shear or slip parallel to bedding.

IC16–300 [P] Half of sample is fine-grained laminated pyrite, other half is mostly coarse pyrite, cemented by quartz and micas and by late marcasite.

IC16–306 [P,C] Pyritic disruption zone, nonmagnetic. Wallrock is lumpy argillite and siltite.

IC16–311 [C] Pyritic infilling of disruption zone, pyrite finer than in IC16–306; sulfides are layered parallel to adjacent bedding, caused by slump or slide(?).

IC16–336 [C] Undisturbed laminated siltite and argillite footwall to disrupted sequence, generally low sulfide except for some laminae of fine pyrite (pyrite mud?).

IC16–351 [C] Bedded siltite and argillite containing abundant disseminated and laminated fine pyrite.

IC16–542 [C] Quartzite containing layers of magnetite, low sulfide content.

IC18–700 [C] Thinly laminated siltite, collected for background reference.

IC18–729 [P] Disrupted siltite and argillite having lumpy texture; carbonate-quartz-pyrite fill ovoids and replace argillite; muscovite and biotite (altered to chlorite) abundant in disruptions.

IC18–762 [P, C] Thin disruption structure 3 cm thick cuts lumpy clay-pyrite rock; pyrite replaces micas and is cemented by quartz.

IC18–767 [C] Disruption zone having high sulfide content, averaging about 40 percent, some of which is veinlike.

IC18–768 [C] Split of sample IC18–768.

IC18–770 [P,C] Small sample very rich in pyrite, about 70 percent over a 0.6-m length, and assay indicated high arsenic content, about 0.25 percent; massive euhedral pyrite, minor marcasite, late anhedral pyrite (composition indicated by SEM-EDS analysis).

IC18–776 [P] Laminated siltite and quartzite containing layers of fine pyrite and a phosphate mineral(?), well-crystallized biotite and muscovite, cemented by quartz.

IC18–781 [P,C] Laminated argillite and siltite cut by thin disruptions filled by quartz-carbonate-pyrite.

IC18–854 [C] Faintly laminated fine quartzite.

IC18–861 [P] Siltite cut by 2-cm break filled by coarse pyrite and magnetite.

IC18–862 [P] Siltite cut by 1-cm break filled by quartz-pyrite-magnetite; wallrock contains much more pyrite than magnetite, break contains about equal amounts of pyrite and magnetite.

IC18–887 [P] Laminated argillite and siltite cut by 2-cm break filled by quartz-pyrite-magnetite; wallrocks contain more magnetite than pyrite.

IC18–894 [P] Altered dike: carbonate and quartz alteration, elongate plagioclase phenocrysts, muscovite-biotite-chlorite-magnetite matrix.

IC18–1064 [C] Bedded siltite containing little sulfide, a few narrow disruptions.

IC18–1068 [P,C] Bedded siltite and argillite above disruption zone, low sulfide content.

IC18–1072 [P] Laminated siltite and argillite containing stringers of quartz-pyrite-magnetite and having no alteration selvage along stringers; quartz is sand-sized (100–200 μm) mosaic of interlocked grains having no apparent detrital shapes.

IC18–1074 [P,C] Thoroughly disrupted zone, rare beds survive; thick layers (as much as 25 cm) of pyrite and magnetite; some layers of fine magnetite and pyrite have appearance of clastic beds.

IC18–1079 [C] Laminated siltite below disruption zone, rich in fine-grained laminated pyrite.

IC18–1080 [C] Laminated siltite and fine quartzite in which there are only a few small disruptions; low sulfide content, moderately magnetic.

IC18–1081 [C] Sawn split of IC18–1080, above.

APPENDIX 2. METHODS FOR GEOCHEMICAL ANALYSIS

Rock samples were analyzed by chemists of the U.S. Geological Survey using standard methods described below. For more information consult the references cited. Limits of detection are summarized in table 3.

X-ray fluorescence (XRF): Sample (0.8 g) is fused in lithium tetraborate, and the glass disk is analyzed for major elements by wavelength-dispersive X-ray spectrometry. J.E. Taggart and A.J. Bartel, analysts. The method is described by Taggart and others (1987).

Induction-coupled plasma–atomic-emission spectrometry (ICP): Sample (0.2 g) is digested with mixed acids (HF, HCl–HNO_3, $HClO_4$) to dryness, then redissolved in HCl–HNO_3 and then analyzed by induction-coupled plasma–atomic-emission spectrometry for which lutetium is an internal standard (Lichte and others, 1987). A few refractory minerals are not dissolved by this acid attack; specifically, for B in tourmaline and Zr in zircon, the sample is sintered in Na_2O_2 prior to ICP analysis for B and Zr. Paul Briggs, analyst.

Special element analysis: Six additional elements were analyzed on request as determined below. L.L. Jackson, E.E. Engleman, D.B. Hatfield, and E. Brandt, analysts. Methods are described by Jackson and others (1984) and Wilson and others (1987).

Fe as FeO: Sample (0.5 g) is decomposed with HF and H_2SO_4, and the digestate is immersed in a solution of boric, sulfuric, and phosphoric acids. Fe(II) is determined by potentiometric titration using potassium dichromate.

H_2O: Sample (1.0 g) is heated at 110 °C for 1 hour, and H_2O^- is determined by weight loss. H_2O^- determined on 0.05-g sample heated with lead oxide and lead chromate, the evolved water analyzed by coulometric Karl Fischer titration.

C, total: Sample (0.75 g) is mixed with Al_2O_3 and combusted in an oxygen atmosphere; total C is determined as CO_2 by infrared absorption spectrometry.

S, total: Sample (0.25 g) mixed with vanadium pentoxide and combusted at 1370°C in oxygenated atmosphere; total S determined as SO_2 by infrared-absorption spectrometry.

Au: Sample (10 g) is digested with HBr–Br_2 and Au extracted with methyl-isobutyl ketone. After washing the organic phase with 0.1M HBr to remove iron, Au is determined by flame atomic-absorption spectrometry (Hubbert and Chao, 1985).

Se: Sample (0.3 g) is digested with $K_2S_2O_8$, HF, HNO_3, and $HClO_4$ followed by a second treatment by HNO_3 and $HClO_4$ combined with H_2SO_4. Solution is mixed with sodium borohydride, and resultent metal hydride is carried in an argon stream into a heated quartz glass tube and determined by atomic-absorption spectrometry.

Table 3. Lower limits of determination in geochemical analyses of samples from the No-Name deposit, Lemhi County, Idaho

[$FeTO_3$, total iron reported as Fe_2O_3. (S) determined by inductively coupled plasma–atomic-emission spectrometry]

Major elements, in weight percent	
SiO_2	0.05
Al_2O_3	.10
$FeTO_3$	.04
FeO	.01
MgO	.10
CaO	.05
Na_2O	.15
K_2O	.02
Fe (S)	.05
Mg (S)	.005
Ca (S)	.05
TiO_2	.02
P_2O_5	.05
MnO	.02
H_2O^+	.01
H_2O^-	.01
C total	.01
S total	.01
Ti (S)	.002
Na (S)	.005
K (S)	.05
P (S)	.005
Minor elements, in parts per million	
Ag	2
As	10
Au	.05
B	20
Ba	1
Be	1
Bi	10
Cd	2
Ce	4
Co	1
Cr	1
Cu	1
Eu	2
Ga	4
Ho	4
La	2
Li	2
Mn	4
Mo	2
Nb	4
Nd	4
Ni	2
Pb	4
Sc	2
Se	.01
Sn	10
Sr	2
Ta	40
Th	4
V	2
Y	2
Yb	1
Zn	2
Zr	8

U.S. GOVERNMENT PRINTING OFFICE: 1989—673-047/86,098 REGION NO. 8

SELECTED SERIES OF U.S. GEOLOGICAL SURVEY PUBLICATIONS

Periodicals

Earthquakes & Volcanoes (issued bimonthly).
Preliminary Determination of Epicenters (issued monthly).

Technical Books and Reports

Professional Papers are mainly comprehensive scientific reports of wide and lasting interest and importance to professional scientists and engineers. Included are reports on the results of resource studies and of topographic, hydrologic, and geologic investigations. They also include collections of related papers addressing different aspects of a single scientific topic.

Bulletins contain significant data and interpretations that are of lasting scientific interest but are generally more limited in scope or geographic coverage than Professional Papers. They include the results of resource studies and of geologic and topographic investigations; as well as collections of short papers related to a specific topic.

Water-Supply Papers are comprehensive reports that present significant interpretive results of hydrologic investigations of wide interest to professional geologists, hydrologists, and engineers. The series covers investigations in all phases of hydrology, including hydrogeology, availability of water, quality of water, and use of water.

Circulars present administrative information or important scientific information of wide popular interest in a format designed for distribution at no cost to the public. Information is usually of short-term interest.

Water-Resources Investigations Reports are papers of an interpretive nature made available to the public outside the formal USGS publications series. Copies are reproduced on request unlike formal USGS publications, and they are also available for public inspection at depositories indicated in USGS catalogs.

Open-File Reports include unpublished manuscript reports, maps, and other material that are made available for public consultation at depositories. They are a nonpermanent form of publication that may be cited in other publications as sources of information.

Maps

Geologic Quadrangle Maps are multicolor geologic maps on topographic bases in 7 1/2- or 15-minute quadrangle formats (scales mainly 1:24,000 or 1:62,500) showing bedrock, surficial, or engineering geology. Maps generally include brief texts; some maps include structure and columnar sections only.

Geophysical Investigations Maps are on topographic or planimetric bases at various scales; they show results of surveys using geophysical techniques, such as gravity, magnetic, seismic, or radioactivity, which reflect subsurface structures that are of economic or geologic significance. Many maps include correlations with the geology.

Miscellaneous Investigations Series Maps are on planimetric or topographic bases of regular and irregular areas at various scales; they present a wide variety of format and subject matter. The series also includes 7 1/2-minute quadrangle photogeologic maps on planimetric bases which show geology as interpreted from aerial photographs. Series also includes maps of Mars and the Moon.

Coal Investigations Maps are geologic maps on topographic or planimetric bases at various scales showing bedrock or surficial geology, stratigraphy, and structural relations in certain coal-resource areas.

Oil and Gas Investigations Charts show stratigraphic information for certain oil and gas fields and other areas having petroleum potential.

Miscellaneous Field Studies Maps are multicolor or black-and-white maps on topographic or planimetric bases on quadrangle or irregular areas at various scales. Pre-1971 maps show bedrock geology in relation to specific mining or mineral-deposit problems; post-1971 maps are primarily black-and-white maps on various subjects such as environmental studies or wilderness mineral investigations.

Hydrologic Investigations Atlases are multicolored or black-and-white maps on topographic or planimetric bases presenting a wide range of geohydrologic data of both regular and irregular areas; principal scale is 1:24,000 and regional studies are at 1:250,000 scale or smaller.

Catalogs

Permanent catalogs, as well as some others, giving comprehensive listings of U.S. Geological Survey publications are available under the conditions indicated below from the U.S. Geological Survey, Books and Open-File Reports Section, Federal Center, Box 25425, Denver, CO 80225. (See latest Price and Availability List.)

"Publications of the Geological Survey, 1879-1961" may be purchased by mail and over the counter in paperback book form and as a set of microfiche.

"Publications of the Geological Survey, 1962-1970" may be purchased by mail and over the counter in paperback book form and as a set of microfiche.

"Publications of the U.S. Geological Survey, 1971-1981" may be purchased by mail and over the counter in paperback book form (two volumes, publications listing and index) and as a set of microfiche.

Supplements for 1982, 1983, 1984, 1985, 1986, and for subsequent years since the last permanent catalog may be purchased by mail and over the counter in paperback book form.

State catalogs, "List of U.S. Geological Survey Geologic and Water-Supply Reports and Maps For (State)," may be purchased by mail and over the counter in paperback booklet form only.

"Price and Availability List of U.S. Geological Survey Publications," issued annually, is available free of charge in paperback booklet form only.

Selected copies of a monthly catalog "New Publications of the U.S. Geological Survey" available free of charge by mail or may be obtained over the counter in paperback booklet form only. Those wishing a free subscription to the monthly catalog "New Publications of the U.S. Geological Survey" should write to the U.S. Geological Survey, 582 National Center, Reston, VA 22092.

Note.—Prices of Government publications listed in older catalogs, announcements, and publications may be incorrect. Therefore, the prices charged may differ from the prices in catalogs, announcements, and publications.